THESIS APPROVAL

GRADUATE SCHOOL, KASETSART UNIVERSITY

Master of Engineering (Information and Communication Technology for Embedded Systems)

DEGREE

Information and Communication Technology for Embedded Systems | Electrical Engineering

FIELD | **DEPARTMENT**

TITLE: A Localization Algorithm Based on Markov Random Field Model for a Stationary Wireless Sensor Network

NAME: Ms. Rattikar Punviset

THIS THESIS HAS BEEN ACCEPTED BY

..... **THESIS ADVISOR**

(Assistant Professor Teerasit Kasetkasem, Ph,D.)

..... **THESIS CO-ADVISOR**

(Ms. La-or Kovavisasuch, Ph,D.)

..... **THESIS CO-ADVISOR**

(Associated Professor Tsuyoshi Isshiki, Ph,D.)

..... **DEPARTMENT HEAD**

(Assistant Professor Teerasit Kasetkasem, Ph.D.)

APPROVED BY THE GRADUATE SCHOOL ON .....

..... **DEAN**

(Associate Professor Gunjana Theeragool, D.Agr.)

THESIS

A LOCALIZATION ALGORITHM BASED ON MARKOV RANDOM FIELD MODEL FOR A STATIONARY WIRELESS SENSOR NETWORK

RATTIKAR PUNVISET

A Thesis Submitted in Partial Fulfillment of
the Requirements for the Degree of
Master of Engineering (Information and Communication Technology for Embedded Systems)
Graduate School, Kasetsart University
2012

Rattikar Punviset 2012: A Localization Algorithm Based on Markov Random Field Model for a Stationary Wireless Sensor Network. Master of Engineering (Information and Communication Technology for Embedded Systems), Major Field: Information and Communication Technology for Embedded Systems, Department of Electrical Engineering. Thesis Advisor: Assistant Professor Teerasit Kasetkasem, Ph.D. 89 pages.

The localization is one of the most important problems for the deployment of wireless sensor networks, especially when the number of sensor nodes is large. The received signal strength (RSS) based localization algorithm is proposed in this work. Here, the RSSs from neighboring sensors are assumed to be statistically dependent. We propose the use of Markov random field to model the correlation of received signal strength of neighboring nodes and to explain this dependency. The maximum likelihood estimate based on this model has been also developed. With this model, our experiment has shown that our proposed algorithm can improve the localization accuracy the localization error can be improved over the traditional localization algorithm without neighboring nodes' information.

_____ _____ __ / __ / __

Student's signature Thesis Advisor's signature

ACKNOWLEDGEMENTS

I would like to grateful thank and deeply indebted Dr. La-or Kovavisaruch who is my thesis advisor from National Electronics and Computer Technology Center, Assistant Professor Dr. Teerasit Kasetkasem who is my thesis advisor from Kasetsart University and Associate Professor Dr. Tsuyoshi Isshiki who is my thesis advisor from Tokyo Institute of Technology for advice, encouragement and valuable suggestion for completely writing of thesis.

This work is supported in part by the grant from Kasetsart University Research and Development Institute (KURDI 2010), Thailand Advanced Institute of Science and Technology (TAIST), National Science and Technology Development Agency (NSTDA), Tokyo Institute of Technology (Tokyo Tech), The Graduate School, Kasetsart University (KU) granted under the research topic ‘A Localization algorithm in a wireless sensor network’.

Rattikar Punviset

September 2012

TABLE OF CONTENTS

Page

LIST OF TABLES

LIST OF TABLES (Continued)

LIST OF FIGURES

LIST OF FIGURES (Continued)

Appendix Figure

LIST OF FIGURES (Continued)

THE SENSOR LOCALIZATION SYSTEM BASED ON MARKOV RANDOM FIELD MODEL FOR A STATIONARY WIRELESS SENSOR NETWORK

INTRODUCTION

A typical wireless sensor network (Stankovic, 2006) is a collection of nodes organized into a cooperative network system. It may contain hundreds or even thousands sensor nodes which spread in a wide area. Each node consists of processing unit (one or more microcontrollers, CPUs or DSP chips), multiple types of memory (program, data and flash memories), a RF transceiver (usually with a single omni-directional antenna), a power source (e.g., batteries and solar cells), and various sensors and actuators. The nodes communicate wirelessly and often self-organize after being deployed in an ad-hoc fashion. Systems of thousands or even ten-thousands nodes are anticipated. These sensor nodes may be deployed in the harsh and difficult terrains which may be difficult to access. For example, sensor nodes may be used in hurricane, volcano, and forest fire areas (Ray *et al*., 2004). Some of these important tasks cannot be implemented without a complete knowledge of sensor node locations. The knowledge of sensor node locations results in the optimum design of network topology and communication route which enable a WSN to become power efficient and have longer lifetime.

In this research, a WSN is used for estimate the position of wireless sensor network. The imperfections in the wireless communication channel between transmitting and receiving nodes are cooperatively estimated. We treat these imperfections as a “noise” in the received signal strength (RSS). Since the transmission from sensor nodes locating in each other proximities to the same receiving node are likely to suffer from the similar level of fading and multipath since both sensors are surrounded by the same environment. Hence, the noise terms in RSSs from packets transmitted from neighboring sensor and measured at a sensor node are assumed to be statistically correlated. Here, the Markov Random Field (MRF) model

is used to capture this statistical dependency. Based on the MRF model, the optimum localization algorithm is developed. The experiment with Tmote sky sensor nodes has also been carried out where our proposed algorithm shows the significant improvement in term of localization accuracy over other localization algorithms without cooperation between neighboring nodes.

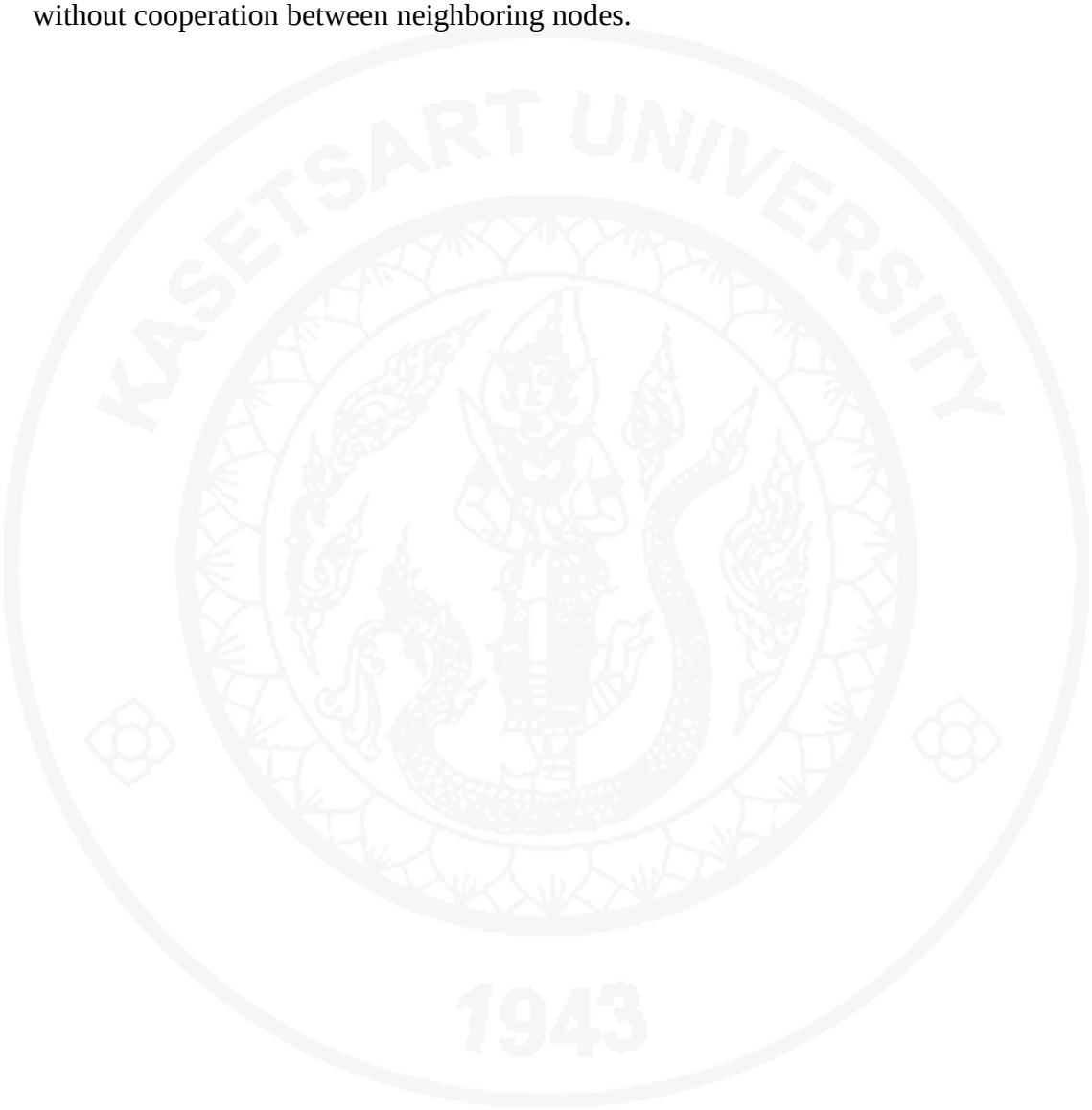

OBJECTIVES

This research has the purposes as shown below:

1. To use the RSSI for joint estimate a sensor node location n WSN

2. To study the effect when the elevation of emitter and antenna of emitter node has a different direction.

LITERATURE REVIEW

In this chapter, the significance of wireless sensor networks and the mathematical models is used for localization are reviewed. We begin the chapter by introducing the localization such that GPS and WSN following by the review of the some of the existing localization technique in WSN. Next, we discuss two mathematical models, namely the linear regression and Markov Random Field models to make this thesis self-contained.

1. Global Positioning System (GPS)

The global positioning system (GPS) is the most widely used devices for determining location. (Kline, 1997) It has a constellation of 24 satellites, in circular orbits around Earth and distributed in six orbital planes equally spaced in 60˚ angle apart and each containing four satellites. The inclination of the orbital plane with respect to the equator is 55˚ in order to provide global coverage. Each orbit is nearly circular with an eccentricity close to zero (< 0.02). The orbital period of 11 hrs. 58 min allows for the use of Doppler frequency shift which occurs due to relative motion. Such carrier phase measurements can be used along with the transmitted pseudorandom noise codes to improve accuracy. Each satellite carries an operating atomic clock (along with several backup clocks) and emits times signals that include a code containing its location. By analyzing signals from at least four of these satellites, a receiver on the surface of the Earth with a built-in microprocessor can display the location of the receiver (latitude, longitude, and altitude). The receiver uses delay lock loops (DLLs) to correlate incoming bit sequences with identical sequences generated by the receiver. The bit sequences are Gold codes Edwin (Taylor**,** 2003) formed as a product of pseudorandom noise sequences. By aligning the received and locally generated codes, the receiver determines the pseudo range to each satellite. When the measurement is made, the receiver clock time is compared to the satellite time of transmission to determine the pseudo range. The satellite time of transmission is encoded onto the bit sequence using the navigation data and provided a position accurate to hundred meters or so. Military versions decode the signal to provide

position readings that are more accurate—the exact accuracy a military secret. GPS satellites are gradually revolutionizing driving, flying, hiking, exploring, rescuing, and map making. However due to high energy requirement, a GPS receiver is impractical for energy-constrained environment such as a wireless sensor network. A GPS receiver makes the large scale deployment of GPS devices in WSNs impractical and requirement of line of sight between satellites. Hence the localization in sensor network is often based on other approaches.

2. Wireless Sensor Network (WSN)

From the work by Guoqiang M. *et.al* and Rong P.*et.al*, (Guoqiang *et.al*., 2006; Rong *et.al*, 2006) a wireless sensor network (WSN) is a significant technology attracting considerable research interest because recent advances in wireless communications and electronics have enabled the development of low-cost, low-power and multi-functional sensors that are small in size and communicate in short distances. A typical WSN consisting a cheap, smart sensors, networked through wireless links and deployed in large numbers provides unprecedented opportunities for monitoring and controlling homes, cities, and the environment. Self-localization capability is a highly desirable characteristic of wireless sensor networks. The application of WSN is reconnaissance and surveillance in the environment area which is difficult to access. Since in environmental monitoring applications such as bush fire surveillance, water quality monitoring and precision agriculture, the measurement data are meaningless without knowing the location from which the data are obtained. Moreover, location estimation may enable a myriad of applications such as inventory management, intrusion detection, road traffic monitoring, health monitoring, reconnaissance and surveillance.

3. Sensor Localization Algorithm

Sensor network localization algorithms estimate the locations of sensors with initially unknown location information by using knowledge of the absolute positions of a few sensors and inter-sensor measurements such as distance and bearing measurements. Sensors with known location information are called anchors and their locations can be obtained by using a global positioning system (GPS), or by installing anchors at points with known coordinates. In applications requiring a global coordinate system, these anchors will determine the locations of the sensor nodes in the global coordinate system. In applications where a local coordinate system suffices (e.g., smart homes), these anchors define the local coordinate system to which all other sensors are referred. Because of constraints on the cost and size of sensors, energy consumption, implementation environment (e.g., GPS is not accessible in some environments) and the deployment of sensors (e.g., sensor nodes may be randomly scattered in the region), most sensors do not know their locations. These sensors with unknown location information are called non-anchor nodes and their coordinates will be estimated by the sensor network localization algorithm

(Stankovic, 2006) For WSN, which are often deployed in an ad hoc fashion, routing typically begins with neighbor discovery. Nodes send rounds of messages (packets) and build local neighbor tables. These tables include the minimum information of each neighbor's ID and location. This means that nodes must know their geographic location prior to neighbor discovery. Other typical information in these tables include nodes' remaining energy, delay via that node, and an estimate of link quality. Node localization is the problem of determining the geographical location of each node in the system. Localization is one of the most fundamental and difficult problems that must be solved for WSN. Localization is a function of many parameters and requirements potentially making it very complex.

(Rong *et.al*, 2006) Another technique is to use a limited number of nodes that are aware of their positions. These nodes are referred to as beacons. The rest of the nodes are referred to as unknowns and utilize beacons' positions to localize

themselves. Depending on the mechanisms used, localization schemes can be classified into two categories:

- Range-free or proximity-based.
- Range-based.

The proximity-based or range free schemes infer constraints on the proximity to the beacon nodes. In range-free schemes, distances are not determined directly, but hop counts are used. Once hop counts are determined, distances between nodes are estimated using an average distance per hop, and then geometric principles are used to compute location. Range-free solutions are not as accurate as range-based solutions and often require more messages. However, they do not require extra hardware on every node. Range-based schemes use various techniques to first determine distances between node (range) and then compute location using geometric principles. To determine distances, extra hardware is usually employed, e.g., hardware to detect the time difference of arrival of sound and radio waves. This difference can then be converted to a distance measurement. The range-based schemes rely on the range measurements. Thus, the estimate the locations of sensor nodes by using various information such as the time-of-arrival (TOA), the angle of arrival (AOA), the time difference of arrival (TDOA) and the receive signal strength (RSS).

3.1 Time of Arrival (TOA)

The time of arrival (TOA) (Guoqiang *et.al*., 2006) is known as one-way or roundtrip propagation time measurements. Distances between neighboring sensors can be estimated from these propagation time measurements. The TOA as commonly used in most radar and sonar systems. Due to the nature of a short range communication in most WSNs, the TOA approaches can only be implemented with addition devices such as ultrasonic microphones and speakers. In general, the TOA provides very high positioning accuracy. One-way propagation time measurements measure the difference between the sending time of a signal at the transmitter and the receiving time of the signal at the receiver. It requires the local times at the transmitter

and the receiver to be accurately synchronized. This requirement may be added to the cost of sensors by demanding a highly accurate clock and/or increase the complexity of the sensor network by demanding a sophisticated synchronization mechanism. This disadvantage makes one-way propagation time measurements a less attractive option than measuring roundtrip time in WSNs. Roundtrip propagation time measurements measure the difference between the time when a signal is sent by a sensor and the time when the signal returned by a second sensor is received at the original sensor. Since the same clock is used to compute the roundtrip propagation time, there is no synchronization problem. The major error source in roundtrip propagation time measurements is the delay required for handling the signal in the second sensor. This internal delay is either known via a priori calibration, or measured and sent to the first sensor to be subtracted. However, it has very limited range since ultrasonic wave can only travel in the distance of few meters.

3.2 Angle of Arrival (AOA)

The AOA (Guoqiang *et.al*., 2006) is defined as the angle between the propagation direction of an incident wave and some reference direction, which is known as italic. Italic, defined as a fixed direction against which the AOAs are measured, the orientation is represented in degrees in a clockwise direction from the North. One common approach to obtain AOA measurements is to use an antenna array on each sensor node. Each sensor node uses both the position of the beacons and the AOA measurements to estimate its position. The angle-of-arrival measurement techniques can be further divided into two subclasses: those making use of the receiver antenna's amplitude response and those making use of the receiver antenna's phase response.

Beamforming is the name given to the use of anisotropy in the reception pattern of an antenna, and it is the basis of one category of the AOA measurement techniques. The measurement unit can be of small size in comparison with the wavelength of the signals. One can imagine that the beam of the receiver antenna is

rotated electronically or mechanically, and the direction corresponding to the maximum signal strength is taken as the direction of the transmitter. Relevant parameters are the sensitivity of the receiver and the beamwidth. A technical problem to be faced and overcome arises when the transmitted signal has varying signal strength. The receiver cannot differentiate the signal strength variation due to the varying amplitude of the transmitted signal and the signal strength variation caused by the anisotropy in the reception pattern. One approach to deal with the problem is to use a second non-rotating and omnidirectional antenna at the receiver. By normalizing the signal strength received by the rotating anisotropic antenna with respect to the signal strength received by the non-rotating omnidirectional antenna, the impact of varying signal strength can be largely removed. Another widely used approach to cope with the varying signal strength problem is to use a minimum of two (but typically at least four) stationary antennas with known, anisotropic antenna patterns. Overlapping of these patterns and comparing the signal strength received from each antenna at the same time yields the transmitter direction, even when the signal strength changes. Coarse tuning is performed by measuring which antenna has the strongest signal, and it is followed by fine tuning which compares amplitude responses. Because small errors in measuring the received power can lead to a large AOA measurement error, a typical measurement accuracy for four antennas is 10 - 15 degrees (Rong *et.al*,2006.). With six antennas, this can be improved to about 5 degrees, and 2 degrees with eight antennas (Rong *et.al*,2006; Guoqiang *et.al*., 2006).

The second category of measurement techniques, known as phase interferometry, derives the AOA measurements from the measurements of the phase differences in the arrival of a wave front. It typically requires a large receiver antenna (relative to the wavelength of the transmitter signal) or an antenna array. The adjacent antenna elements are separated by a uniform distance *d*. The distance between a transmitter far away from the antenna array and the i^{th} antenna element can be approximated by

$$R_i \approx R_0 - idcos\theta \quad (1)$$

where R_0 is the distance between the transmitter and the zeroth antenna element and θ is the bearing of the transmitter with respect to the antenna array. The transmitter signals received by adjacent antenna elements have a phase difference of $2\pi\frac{d\cos\theta}{\lambda}$, which allows us to obtain the bearing of the transmitter from the measurement of the phase difference. This approach works quite well for high SNR but may fail in the presence of strong co-channel interference and/or multipath signals.

3.3 Time difference of Arrival (TDOA)

(Guoqiang *et.al*, 2006) The TDOA is commonly used in civil and military surveillance applications to accurately locate an aircraft, vehicle or stationary emitter by measuring the TDOA of a signal from the emitter at three or more receiver sites to estimate the location of the transmitter. It also refers to the case of locating a receiver by measuring the TDOA of a signal transmitted from three or more synchronized transmitters. There is a category of localization algorithms utilizing the TDOA measurements of the transmitter signal at a number of receivers with known location information to estimate the location of the transmitter. Fig. 1 shows a TDOA localization scenario with a group of four receivers at locations r_1; r_2; r_3; r_4 and a transmitter at r_t. The TDOA between a pair of receivers i and j is given by:

$$\Delta t_{ij} \triangleq t_i - t_j = \frac{1}{c}\left(\|r_i - r_t\| - \|r_j - r_t\|\right), i \neq j \qquad (2)$$

where t_i and t_j are the time when a signal is received at receivers i and j respectively, c is the propagation speed of the signal, and $\|\cdot\|$denotes the Euclidean norm.

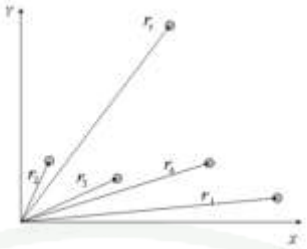

Figure 1 Time difference of arrival receiver and transmitter node (Guoqiang *et.al*., 2006)

3.4 Received Signal Strength Indicator (RSSI)

Another approach for localization in a WSN is to use a received signal strength indicator (RSSI)-based systems. The RSSI is an indication of the signal power received by a receiver from an incoming signal, which is known to be inversely proportional to the distance between a transmitter and a receiver, and depends on distances between transmitters and receivers. A receiver closest to a transmitter should have the highest value of RSSI. The RSSI (Ambili *et.al*., 2009) is defined as ten times the logarithm of the ratio of power of the received signal and a reference power. The RSSI varies ten logarithm proportional between power and reference power (RSSI α 10 log *P/Pref*). This means that the RSSI varies from logarithm of power (RSSI α logP). It is known that power dissipates from a point source as it moves further out, and the relationship between power and distance is that power is inversely proportional to the square of the distance travelled. Hence, the RSSI can potentially be used as an indicator of the distance at which the sending mote is located from the receiving mote. When data from many such neighboring motes are combined, the location of the sending mote can be judged with reasonable accuracy.

Eq. (3) (Zhang *et al*, 2009) is the shadowing model which is widely used in wireless signal transmission,

$$[\overline{p_r(d)}]_{dBm} = [p_r(d_0)]_{dBm} - 10nlog\left(\frac{d}{d_0}\right) + X_{dBm} \quad (3)$$

where in Eq.*(3)*, *d* is the distance from transmitter to receiver and its unit is meter, d_0 is the reference distance and usually equals to one meter, $[\overline{p_r(d)}]_{dBm}$ is the signal power received from the transmitter and its unit is dBm, X_{dBm} is a Gaussian random variable whose mean value is zero and it reflects the change of the received signal power in certain distance, *n* is the path loss index and relates to the environment. When the Gaussian random variable is not considered the formula is shown in formula (4).

$$[\overline{p_r(d)}]_{dBm} = [p_r(d_0)]_{dBm} - 10nlog\left(\frac{d}{d_0}\right) \quad (4)$$

Usually, the simplified version of Eq.*(4)* is shown in Eq.*(5)*.

$$RSSI_{[dBm]} = [\overline{p_r(d)}]_{dBm} = A - 10nlog(d) \quad (5)$$

where *n* is the slope of the standard plot. *n* can be obtained by performing a linear regression analysis on the data points used to generate the standard curve. This analysis could also provide the estimate of the constant parameter *'A'* in the equation that fits the data the best. Further this linear regression fit plot can be used to estimate the distance between two motes for a given RSSI value based on the formula as shown above.

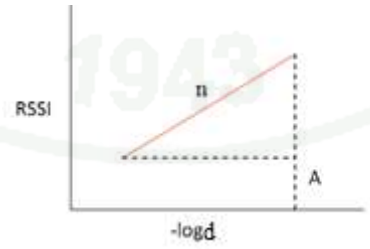

Figure 2 Standard plot of receive signal strength (Ambili *et.al*, 2009)

4. Linear Regression Model

Regression analysis is a statistical tool for the investigation of relationships between two parameters or more. (Potiban, 2010) The regression model is classification in 2 types such that

- The linear regression analysis is the statistically method to analyze the relationship of quantitative variables the independent and dependent variables. The relationship between parameters can be represented by linear equation. The linear regression analysis can be categorize into:
  - The simple linear regression is the linear regression analysis which has one independent variable and one dependent variable to consider and create the mathematical model to predict the value of dependent variable
  - The multiple linear regression has one dependent variable and two or more independent variable to analyze and make the equation to explain the relationship and approximate the value of dependent variable.
- Nonlinear regression analysis is the method for find the relationship of the variables, these variables are nonlinearly and represented by nonlinear model

In this research, the simple linear regression model is used to find the relationship between received signal power and the distance between transmitter and receiver. We consider that (Cottrell, 2003) some variable of interest *y* is driven by some other variable x. The variable *y* will be calling the dependent variable and *x* is the independent variable.

Let *i* be an index the observations on the data pairs (x_i, y_i). The simple linear model formalizes as:

$$y_i = \beta_0 + \beta_1 x_i + \mu_i \quad (6)$$

where the parameter β_0 and β_1 represent the y-intercept and the slope of the relationship, y_i is the dependent variable, x_i is the independent variable and μ_i is the deviation respectively. In Eq.(6), we want to find the coefficient of this formula which calculated from the observation data and coefficient of this formula is find from equation below

$$\hat{y}_i = \hat{\beta}_0 + \hat{\beta}_1 x_i \tag{7}$$

when $\hat{\beta}_0 = \bar{Y} + \hat{\beta}_1 \cdot \bar{X}$ and $\hat{\beta}_1 = r_{xy} \cdot \frac{S_y}{S_x}$ where r_{xy} is $\frac{N\sum XY - (\sum X)(\sum Y)}{\sqrt{[N\sum X^2 - (\sum X)^2][N\sum Y^2 - (\sum Y)^2]}}$,($\bar{Y}$, $\bar{X}$) is the average of variable *x* and *y* and (S_y,S_x) is the standard deviation of variable *x* and *y*

5. Markov Random Field Model (MRF)

The Markov random field models (Kasetkasem, 2002) is used to explain various phenomena among neighboring particles and explain why neighboring particles are more likely to rotate in the same direction (clockwise or counterclockwise) or why intensity value of adjacent pixels of an image are more likely to be the same than different and obvious that this type of spatial dependence. The MRF is a common phenomenon in various signal type, and have been used by statistical physicists to explain various phenomena among neighboring particles because of their ability to describe local interaction between them. Basically, an MRF model is a spatial-domain extension of a temporal Markov chain where an event at the current time instant depends only on event of a few previous time instants. In the MRF, the statistical dependence is defined over the neighborhood system, a collection of neighbors, rather than past events as in the Markov chain model. It is obvious that this type of spatial dependence is a common phenomenon in various signal type including image. In this research, the pixel is represented by small area or grid and considers the interesting area look like the image and the intensity noise values of neighboring grids are highly dependent on each other.

Discrete image (Winkler, 2003) was representing by element of finite product spaces and special probability distributions on the set of such images were discussed. And appropriate abstract setting will now be introduced.

Let $\mathcal{S} = \{s_1, s_2, \dots, s_M\}$ be a finite index set. The finite index set is the set of sites; for every site $s \in \mathcal{S}$ letX_s be a finite space of state x_s. When the *X* and *Y* is the vector which represented by observer image. The product $X = \prod_{s\in\mathcal{S}} X_s$ is the space of (finite) configuration $x = (x_s)_{s\in\mathcal{S}}$. Subsets $E \subset X$ are call event; the probability of an event E is given by $\Pr(E) = \sum_{x\in E} \Pr(x)$. A strictly positive probability measure probability on *X*, i.e. $\Pr(x) > 0$ for every $x \in X$, is call a stochastic or random field. For $A \subset \mathcal{S}$ let $X_A = \prod_{s\in\mathcal{S}} X_s$ denote the space of configurations $x_A = (x_s)_{s\in A}$on A; the map is the projection of *X* onto X_A.

$$X_A: X \to X_A, x = (x_s)_{s\in S} \leftrightarrow (x_s)_{s\in A} \tag{8}$$

The short-hand notation is used for X_s for $X_{\{s\}}$ and $\{X_A = x_A\}$ for $\{x \in X: X_A(x) = x_A\}$. Commonly one write $\{X_A = x_A, X_B = x_B\}$ for intersection $\{X_A = x_A\} \cap \{X_B = x_B\}$. For a random field Ω the random vector $X = (X_s)_{s\in\mathcal{S}}$ on the probability space (X,Ω) is also frequently called a random field.

For events *E* and *F* the conditional probability of *F* given *E* is defined by $\Pr(F|E) = \Pr(F \cap E)/\Pr(E)$. Conditional probabilities of the form

$$\pi^s(x) = Pr\left(X_A = x_A \middle| X_{\mathcal{S}\setminus A} = x_{\mathcal{S}\setminus A}\right), A \subset \mathcal{S}, x_A \in X_A, x_{\mathcal{S}\setminus A} \in X_{\mathcal{S}\setminus A}, \tag{9}$$

are called local characteristics. They are always defined since random field are assumed to be strictly positive. They express the probability that the configuration is $x_A$on A and $x_{\mathcal{S}\setminus A}$on the rest of the world.

The index set $\mathcal{S}$ is a finite square lattice and $\langle s,t\rangle$ means that *t* is the site next to *s* on the right or left or the next upper or lower site (or more generally, $\mathcal{S}$ is a finite

undirect graph with bonds $\langle s,t \rangle$).A collection $\partial = \{\partial(s): s \in \mathcal{S}\}$ of subset of $\mathcal{S}$ is call a neighborhood system, if $(i)\ s \notin \partial(s)$ and $(ii)\ s \in \partial(t)$. The site $s \in \partial(t)$ are call neighbors of *t*. A subset *C* of $\mathcal{S}$ is call a clique if two different element of *C* are always neighbor. The set of clique will be denoted by *C*. We shall frequently write $\langle s,t \rangle$ if *s* and *t* are neighbors of each other.

The neighborhood relation induces an undirected graph with vertices $s \in \mathcal{S}$ and bond between *s* and *t* if and only if *s* and *t* are neighbors. Conversely, a directed graph induces a neighborhood system. The 'complete' set in the graph correspond to the cliques.

The random field *X* is a Markov field with reference to the neighborhood system ∂ if for all $x \in X$,

$$Pr(X_s = x_s | X_r = x_r, r \neq s) = Pr(X_s = x_s | X_r = x_r, r \in \partial(s)) \qquad (10)$$

The Gibbsian form is a particularly useful for the calculation of (conditional) probabilities. The idea and hence most of the terminology is borrowed from statistical mechanics where Gibbs fields are used as model for the equilibrium states of large physical systems. Probability measures of the form

$$\pi = Pr(x) = \frac{\exp(-H(x))}{\sum_{z \in X} \exp(-H(z))} \qquad (11)$$

are always strictly positive and hence random fields. π is called the Gibbs field (or measure) induced by the energy function *H* and the numerator is called the partition function. Every random field π can be written in this form. In fact, setting *H(x) = -ln(Pr(x))-ln(Z)*, one gets *exp(-H(x)) = Pr(x)Z* and *Z* necessarily is the partition function of *H*. Moreover, the energy function for π is unique up to an additive constant; if *H* and *H'* are energy function for π then

$$H(x) - H'(x) = lnZ' - lnZ \qquad (12)$$

for every $x \in X$. It is common to enforce uniqueness choosing some reference or 'vacuum' configuration $o \in X$ and requiring $Z = \pi(o)^{-1}$, or, equivalently $H(o) = 0$

A potential is a family $\{U_A : A \subset \mathcal{S}\}$of functions on X such that

(i)$U_\emptyset = 0$; ϕ is the empty set

(ii)$U_A(x) = U_A(y)\ if\ X_A(x) = X_A(y)$

The energy of the potential *U* is given by

$$H_U = \sum_{A \subset S} U_A \tag{13}$$

Given a neighborhood system ∂ a potential *U* is called a neighbor potential with reference to ∂ if $U_A = 0$ whenever *A* is not a clique. If $U_A = 0$ for $|A| > 2$ then *U* is a pair potential. Potential define energy functions and random fields.

If a Markov field is given by a potential then the local characteristics may easily be calculated. Let the random field π be given by some neighbor potential *U* for the neighborhood system ∂, i.e.

$$\pi = Pr(x) = \frac{\exp(-\sum_{c \in C} U_c(x))}{\sum_y exp(-\sum_{c \in C} U_c(y))} \tag{14}$$

where *C* denotes the set of cliques of ∂. Then the local characteristics are given by

$$Pr\left(X_s = x_s, s \in A \middle| X_S = x_S, s \in S \backslash A\right) = \frac{\exp(-\sum_{c \in C, c \cap A \neq \emptyset} U_c(x))}{\sum_{y_A \in X_A} exp(-\sum_{c \in C, c \cap A \neq \emptyset} U_c(y))} \tag{15}$$

$$Pr\left(X_s = x_s, s \in A \middle| X_S = x_S, s \in S \backslash A\right) = Pr\left(X_s = x_s, s \in A \middle| X_S = x_S, s \in \partial(A)\right) \tag{16}$$

for every subset *A* of $\mathcal{S}$. In particular, π is a Markov field with reference to ∂.

6. Expectation Maximization Algorithm (EM Algorithm)

The EM algorithm (Borman, 2009) is an efficient iterative procedure to approximate the Maximum Likelihood (ML) estimate in the presence of missing or hidden data. In ML estimation, we wish to estimate the model parameter(s) for which the observed data are the most likely. Each iteration of the EM algorithm consists of two processes: The expectation (E) step, and the maximization (M) step. In the expectation step, or E-step, the hidden data are estimated given the observed data and current estimate of the model parameters. The approximate distribution of the hidden data from the E-step are used in represent of the actual hidden data. This is achieved using the conditional expectation, explaining the choice of terminology. In the M-step, the likelihood function is maximized expectation data from E-step. Convergence is assured since the algorithm is guaranteed to increase the likelihood at each iteration.

Let X be random vector which results from a parameterized family. We wish to find θ such that Pr(X|θ) is a maximum. This is known as the Maximum Likelihood (ML) estimate for θ. In order to estimate θ, it is typical to introduce the log likelihood function defined as,

$$L(\theta) = \ln Pr(X|\theta) \tag{17}$$

The likelihood function is considered to be a function of the parameter θ given the data X. Since ln(x) is a strictly increasing function, the value of θ which maximizes Pr(X|θ) also maximizes $L(\theta)$. The EM algorithm is an iterative procedure for maximizing $L(\theta)$. Assume that after the n^{th} iteration the current estimate for θ is given by θ_n. Since the objective is to maximize $L(\theta)$, we wish to compute an updated estimate θ such that,

$$L(\theta) > L(\theta_n) \tag{18}$$

Equivalently we want to maximize the difference,

$$L(\theta) - L(\theta_n) = \ln Pr(X|\theta) - \ln Pr(X|\theta_n) \tag{19}$$

So far, we have not considered any unobserved or missing variables. In problems where such data exist, the EM algorithm provides a natural framework for their inclusion. Alternately, hidden variables may be introduced purely as an artifice for making the maximum likelihood estimation of θ tractable. In this case, it is assumed that knowledge of the hidden variables will make the maximization of the likelihood function easier. Either way, denote the hidden random vector by *Z* and a given realization by *z*. The total probability Pr(X|θ) may be written in terms of the hidden variables *z* as,

$$Pr(X|\theta) = \sum_z Pr(X|z,\theta)Pr(z|\theta) \tag{20}$$

EM algorithm thus consists of iterating the:

- E-step: Determine the conditional expectation $E_{Z|X,\theta_n}\{\ln P\,(X|z,\theta)\}$ and compute the conditional expectation (with respect to the missing *y*) of the logarithm of the complete a posteriori probability function,
- M-step: Maximize this expression with respect to θ.

So, we may rewrite Eq. *(19)* as:

$$\begin{aligned} L(\theta) - L(\theta_n) &= \ln\Big(\sum_x \Pr(X|z,\theta)\, P(z|\theta)\Big) - \ln Pr(X|\theta_n) \\ &\triangleq \Delta(\theta|\theta_n) \end{aligned} \tag{21}$$

After that, we discuss the general convergence of the algorithm. Recall that θ_{n+1} is the estimate for θ which maximizes the difference $\Delta(\theta|\theta_n)$. Starting with the current estimate for θ, that is, θ_n we had that $\Delta(\theta_n|\theta_n) = 0$. Since θ_{n+1} is chosen to maximize$\Delta(\theta|\theta_n)$, we then have that $\Delta(\theta_{n+1}|\theta_n) \geq \Delta(\theta_n|\theta_n) = 0$, so for each iteration the likelihood $L(\theta)$ is nondecreasing.

In the formulation of the EM algorithm described above, θ_{n+1} was chosen as the value of θ for which $\Delta(\theta|\theta_n)$. was maximized. While this ensures the greatest

increase in $L(\theta)$, it is however possible to relax the requirement of maximization to one of simply increasing $\Delta(\theta|\theta_n)$. so that $\Delta(\theta_{n+1}|\theta_n) \geq \Delta(\theta_n|\theta_n)$. This approach, to simply increase and not necessarily maximize $\Delta(\theta_{n+1}|\theta_n)$ is known as the Generalized Expectation Maximization (GEM) algorithm and is often useful in cases where the maximization is difficult. The convergence of the GEM algorithm can be argued as above.

7. Related Work

In recent years, there is research work which studied the localization problem in wireless sensor networks. Each research work has different purpose such as use difference method for detecting, reduce power of sensor, increase efficiency etc. For example, Sigma-Point Kalman Smoothers (Anindya, 2009) is employed for finding a location and velocity of sensor node. In their work, the researchers used the forward–backward statistically linearized sigma-point Kalman smoother (FBSL-SPKS) and fixed-lag sigma-point Kalman smoother (FL-SPKS) algorithms for tracking purposes. Both the FBSL-SPKS and FL-SPKS estimators fuse a model of walking motion, room–wall configurations and all available sensor observations in order to track a person and use recursive Bayesian estimation which is a general probabilistic approach for sequentially estimating an unknown state probability density function over time using incoming noisy measurements and a mathematical process model. The problem can often be casted in terms of estimating the state of a discrete-time nonlinear dynamic system. In (Sundaresan *et al.*, 2011) the correlated of observation sensor is employed to estimate the location. The researchers focus on a source emitting a random signal and present an MLE (Maximum Likelihood Estimator) for estimation location by assuming that the marginal likelihoods of sensor observations does not need to be identical and the joint likelihood function of observations is unknown. System design is usually carried out by enforcing the assumption of conditional independence using the joint likelihood function which can be written as a product of individual marginal likelihood functions. The model selection techniques for data-driven copula function selection and a model fusion strategy to enhance the performance of the copula based location estimator are used in this research. Copula

based approximation of the joint likelihood function to perform MLE using observations from different sensors and improving the overall estimation performance by fusing the location estimates resulting from the use of different copula functions, employing model selection techniques.

MATERIALS AND METHODS

This chapter is started by materials used in this study. Then, the methods of investigation and implementation of proposed approach are presented.

Materials

The experiments of study about sensor localization problem, the sensor node is very important. In this work, the Tmote sky board mote *IV* is used for the experiment.

1. Tmote Sky (Lorincz, 2006) is an ultra-low power wireless module for use in sensor networks, monitoring applications, and rapid application prototyping. The feature of Tmote sky is:

- 250kbps 2.4GHz IEEE 802.15.4 Chipcon Wireless Transceiver
- Interoperability with other IEEE 802.15.4 devices
- 8MHz Texas Instruments MSP430 microcontroller (10k RAM, 48k Flash)
- Integrated ADC, DAC, Supply Voltage Supervisor, and DMA Controller
- Integrated onboard antenna with 50m range indoors / 125m range outdoors
- Integrated Humidity, Temperature, and Light sensors
- Ultra low current consumption
- Fast wakeup from sleep (<6μs)
- Hardware link-layer encryption and authentication
- Programming and data collection via USB
- 16-pin expansion support and optional SMA antenna connector
- TinyOS support : mesh networking and communication implementation
- Complies with FCC Part 15 and Industry Canada regulations

Figure 3 Tmote sky board mote *IV*
(Lorincz, 2006)

2. The MATLAB is used for finding the solution of the model. The MATLAB version 7.11.0 (2010b) is useful for calculating the equation and finds the optimum parameter to reduce the error

Methods

1. Problem statement

In this section, we examine two cases; the first one is the localization when the position of the neighbor in nodes are known and the second one is the only receive signal strength and location of the receiving nodes are known. A sensor node can determine its neighbors by broadcast the beacon message. Any sensor nodes hear this beacon message is a neighbor of the sensor node.

1.1 Received Signal Strength model

In wireless communication channel, the propagating signal is always affected by reflection, diffraction and interference from the surrounding environment, as a result the RSS (Received Signal Strength) is nondeterministic and random in nature. The RSS is often model as lognormal random variable and is given by

$$R_{ij} = R_{0j} - 10n_{ij}\log(\frac{d_{ij}}{d_0}) + P_{ij} \quad (22)$$

where d_{ij} is the distance between Nodes *i* and *j* in meter, d_0 is the reference distance (often it is set at 1 meter), R_{oj} is the RSS at the reference distance in dBm, n_{ij} is the path loss exponent for communication between Nodes *i* and *j*, $P_{ij}$is a random path loss (RPL) caused by the reflections of signal from the surrounding environment in a wireless communication channel.

The triangulation scheme was influenced by the Global Positioning System (GPS), which triangulates the location of a receiver using satellites and the speed of light. Thus we were able to determine the distance between a transmitter node and the receiver node using the lognormal shadowing. The formula below is show the equation method.

$$er(x,y) = \sum_{i=1}^{K}(R_{0j} - 10n_{ij}log\sqrt{[(x_i - a_i)^2 + (y_i - b_i)^2]} - R_{ij})^{\,2} \quad (23)$$

And then, the derivative is used for finding the critical point of this function and the equation is shown below

$$\frac{d}{d(x)}er(x) = \frac{d}{d(x)}\sum_{i=1}^{K}\left(R_{0j} - 5n_{ij}\log[(x_i - a_i)^2 + (y_i - b_i)^2] - R_{ij}\right)^2 = 0$$

$$\frac{d}{d(x)}er(y) = \frac{d}{d(x)}\sum_{i=1}^{K}(R_{0j} - 5n_{ij}log[(x_i - a_i)^2 + (y_i - b_i)^2] - R_{ij})^{\,2} = 0 \quad (24)$$

$$\frac{d}{d(x)}er(x) = \sum_{i=1}^{K}\left[2\left(R_{0j} - 5n_{ij}[(x_i - a_i)^2 + (y_i - b_i)^2] - R_{ij}\right)\cdot\frac{10n_{ij}2((x_i - a_i))}{(x_i - a_i)^2 + (y_i - b_i)^2}\right]$$

$$\frac{d}{d(x)}er(y) = \sum_{i=1}^{K}\left[2\left(R_{0j} - 5n_{ij}[(x_i - a_i)^2 + (y_i - b_i)^2] - R_{ij}\right)\cdot\frac{10n_{ij}2((y - b_i))}{(x_i - a_i)^2 + (y_i - b_i)^2}\right] \quad (25)$$

In this work, we introduce a new idea where the RPL is a combination of from two components which are location dependence and location independence, i.e.,

$$P_{ij} = X_{ij} + W_{ij} \tag{26}$$

Here, X_{ij} and W_{ij} are the location dependence RPL (LDRPL) and location independent RPL (LIRPL) parts of the unknown path loss, respectively. The LDRPL is the part of path loss that is a function of a sensor node locations. Here, we assume that X_{ij} is slowly varied from one sensor to others. In reality, the RSS transmitted by nearby sensor nodes to the same receiver should experience similar level of reflectance, diffraction and interference from multiple paths. In other words,X_{ij} and $X_{ik}$are likely to have similar values and statistically dependent if Nodes j and k are neighbors. Similarly, X_{ij} and X_{kj} can be assume to be also statistically dependent due to the same reason. The LIRPL is the path loss that results from model or measurement errors. Here, we assume that $W_{ij}$is Gaussian random variable with mean of 0 and variance of σ^2, and is independent of the RSS from all other sensor nodes.

In order to characterize this statistical relationship, the Markov random field (MRF) is employed. Let$\boldsymbol{X}_{i\backslash j}$ is the set of the location dependent (LD) parts of the unknown path losses from packets broadcast from all other nodes except not Node *j* to Node *i*. The conditional probability density function (PDF) of X_{ij}given $X_{i\backslash j}$is equal to the conditional PDF ofX_{ij} given the unknown path losses from packet transmitted from the neighboring nodes of Node *j*, i.e.,

$$\Pr\left(X_{ij}\middle|\boldsymbol{X}_{i\backslash j}\right) = \Pr\left(X_{ij}\middle|\boldsymbol{X}_{iN_j}\right) \tag{27}$$

where $\boldsymbol{X}_{iN_j}$ is the set of unknown path losses from packets transmitted from neighboring nodes of Node *j* to Node *i*.. A sensor node can determine its neighbors by broadcast the beacon message. Any sensor nodes hear this beacon message is a neighbor of the sensor node. The MRF properties has the Gibbs distribution whose probability density function depends on configurations of neighboring sites, the marginal PDF of *X* takes the form of Gibbs distribution, i.e.,

$$\Pr(\boldsymbol{X}_i) = \frac{1}{Z} e^{-\sum_{C \in S} V_C(\boldsymbol{X}_i)} \tag{28}$$

where Z is a normalizing constant, S is the set of receiving nodes, C is a clique which is a singleton or any subset of S whose as distinct elements are mutual neighbors, $V_C(\boldsymbol{X})$ is a Gibbs potential function relative to the neighborhood system and $\boldsymbol{X}_i$ is a set of all LDRPLs from all nodes to Node i. The Gibbs potential function is defined by using the unknown path losses from all nodes and the clique. Usually, low values of the potential function correspond to similar values whereas high values correspond to dissimilar values of a clique. In this research, the Gibbs potential function is defined in the quadratic form, i.e.,

$$\sum_{C} V_{\{j,k\}}(X_i) = \sum_{j=1}^{N} \frac{1}{2\beta^2} \left(X_{ij} - \frac{\gamma_i}{\|N_j\|} \sum_{k \in N_j} X_{ik} \right)^2 \tag{29}$$

where $\|N_j\|$ is the number of neighboring nodes of transmitter, and β and γ_i are Gibbs parameters. Here, neighbors are defined as sensor nodes in a predefined communication range.

The maximum likelihood estimator is the method estimation of parameters which is a fundamental problem in data analysis. MLE (Myung, 2003) has many optimal properties in estimation: sufficiency (complete information about the parameter of interest contained in its MLE estimator), consistency (true parameter value that generated the data recovered asymptotically. The principle of maximum likelihood estimation (MLE), originally developed by R.A. Fisher in the 1920s, states that the desired probability distribution is the one that makes the observed data ‘‘most likely’’, which means that one must seek the value of the parameter vector that maximizes the likelihood function.

1.2 The position estimation of single node at a time

In this method, the RSS signal, position of neighbor and position of receiving node are known. The joint probability density function (PDF) of the RSS and the unknown path losses received at Node *i* given all transmitted node locations is given by

$$\mathrm{P_r}\left(R_{ij}, X_{ij} \middle| (x_j, y_j), \boldsymbol{X}_{iN_j}\right) = \mathrm{P_r}\left(R_{ij} \middle| X_{ij}, (x_j, y_j), \boldsymbol{X}_{iN_j}\right) \mathrm{P_r}\left(X_{ij} | \boldsymbol{X}_{iN_j}\right) \quad (30)$$

where $\mathrm{P_r}\left(R_{ij} \middle| X_{ij}, (x_j, y_j), \boldsymbol{X}_{iN_j}\right) = \frac{1}{\sqrt{2\pi\sigma^2}} e^{-\frac{(R_{ij} - \mu_i(x_j y_j) - X_{ij})^2}{2\sigma^2}}$ and $\mathrm{P_r}\left(X_{ij} | \boldsymbol{X}_{iN_j}\right) = \frac{1}{Z} e^{-\sum_{C \in S} V_C(\boldsymbol{x}_i)}$.

Then we have,

$$\mathrm{P_r}\left(R_{ij}, X_{ij} \middle| (x_j, y_j), \boldsymbol{X}_{iN_j}\right) = \mathrm{P_r}\left(R_{ij} \middle| X_{ij}, (x_j, y_j), \boldsymbol{X}_{iN_j}\right) \mathrm{P_r}\left(X_{ij} | \boldsymbol{X}_{iN_j}\right)$$

$$= \frac{1}{\sqrt{2\pi\sigma^2}} e^{-\frac{(R_{ij} - \mu_i(x_j y_j) - X_{ij})^2}{2\sigma^2}} \cdot \frac{1}{Z_{ij}} e^{-\sum_{C \in S} V_C(\boldsymbol{x}_i)}$$

By substituting (29) into the above eq., we have,

$$\mathrm{P_r}\left(R_{ij}, X_{ij} \middle| (x_j, y_j), \boldsymbol{X}_{iN_j}\right) = \frac{1}{\sqrt{2\pi\sigma^2}} e^{-\frac{(R_{ij} - \mu_i(x_j y_j) - X_{ij})^2}{2\sigma^2}} \cdot \frac{1}{Z_{ij}} e^{-\frac{1}{2\beta^2}\left(X_{ij} - \frac{\gamma_i}{\|N_j\|} \sum_{k \in N_j} X_{ik}\right)^2} \quad (31)$$

which can be further written as

$$\Pr\left(R_{ij}, X_{ij} \middle| (x_j, y_j), \boldsymbol{X}_{iN_j}\right) = \frac{\exp\left[-\frac{\left(R_{ij} - \mu_i(x_j, y_j) - X_{ij}\right)^2}{2\sigma^2} - \frac{1}{2\beta^2}\left(X_{ij} - \frac{\gamma_i}{\|N_j\|} \sum_{k \in N_j} X_{ik}\right)^2\right]}{Z_{ij}\sqrt{2\pi\sigma^2}} \quad (32)$$

where Z_{ij} is a normalizing constant and $\mu_i(x_j,y_j) = R_{0j} - 10n_{ij}\,log(\frac{d_{ij}}{d_o})$. Finally, we assume that there are *K* receiving sensor nodes in the system, and the joint PDF of RSSs received at all sensor nodes is given by

$$\mathrm{P_r}\left(\boldsymbol{R}_j, \boldsymbol{X}_j \middle| (x_j,y_j), \boldsymbol{X}_{iN_j}\right) = \prod_{i=1}^{K} \frac{\exp\left[-\frac{\left(R_{ij} - \mu(x_j,y_j) - X_{ij}\right)^2}{2\sigma^2} - \frac{1}{2\beta^2}\left(X_{ij} - \frac{\gamma_i}{\|N_j\|}\sum_{k\in N_j} X_{ik}\right)^2\right]}{Z_{ij}\sqrt{2\pi\sigma^2}} \quad (33)$$

where $\boldsymbol{R}_j = \{R_{1j}, R_{2j}, \ldots, R_{Kj}\}$and $\boldsymbol{X}_j = \{X_{1j}, X_{2j}, \ldots, X_{Kj}\}$ are the sets of RSSs and packets losses of all packets transmitted from Node *j* to all receiving nodes, respectively. Here $\boldsymbol{R}_{ij}$ are assumed to be statistically independent when$\boldsymbol{X}_{ij}$, $\boldsymbol{X}_{ik}$ and positions of sensors are known.

Hence, the marginal PDF of $\boldsymbol{R}_j$ given the location of Node *j* is given

$$\begin{aligned}\Pr\left(\boldsymbol{R}_j \middle| (x_j,y_j), \boldsymbol{X}_{iN_j}\right) &= \int_{-\infty}^{\infty} \Pr\left(\boldsymbol{R}_j, \boldsymbol{X}_j \middle| (x_j,y_j), \boldsymbol{X}_{iN_j}\right) d\boldsymbol{X}_j \\ &= \prod_{i=1}^{K} \frac{1}{\sqrt{2\pi\gamma^2}} \exp\left[-\frac{\left(R_{ij} - \acute{\mu}_i(x_j,y_j)\right)^2}{2\delta^2}\right] \end{aligned} \quad (34)$$

where $\acute{\mu}_i(x_j,y_j) = \mu_i(x_j,y_j) + \frac{\gamma_i}{\|N_j\|}\sum_{k\in N_j} X_{ik}$and $\delta^2 = \sigma^2 + \beta^2$.

Then, the maximum likelihood estimate (ML) is employed to estimate the location of each transmitting nodes. The goal is to find (x_j,y_j) that maximizes$\Pr\left(\boldsymbol{R}_j \middle| (x_j,y_j)\right)$, i.e.,

$$(x_j,y_j)^{opt} = \arg\max_{(x_j,y_j)} \left[\Pr\left(\boldsymbol{R}_j \middle| (x_j,y_j), \boldsymbol{X}_{iN_j}\right)\right]. \quad (35)$$

By taking the derivative of Eq. (34), the optimum solution can be obtained by letting the derivative equation to zero.

In this point, the Eq.33 has an unknown parameter such that X_{ij} ,then we will go back to Eq.(31) and find the mean and variance of X_{ij}.

$$= \frac{\exp\left[-\frac{\left(R_{ij}-\mu_i(x_j,y_j)-X_{ij}\right)^2}{2\sigma^2}-\frac{1}{2\beta^2}\left(X_{ij}-\frac{\gamma_i}{\|N_j\|}\sum_{k\in N_j}X_{ik}\right)^2\right]}{Z_{ij}\sqrt{2\pi\sigma^2}}$$

$$= \frac{\exp\dfrac{\left[\begin{array}{c}\left({R_{ij}}^2-2\mu_i(x_j,y_j)R_{ij}+\mu_i(x_j,y_j)^2-2R_{ij}X_{ij}+2\mu_i(x_j,y_j)X_{ij}+{X_{ij}}^2\right)\\ -2\sigma^2\frac{1}{2\beta^2}\left({X_{ij}}^2-2\frac{\gamma_i}{\|N_j\|}\sum_{k\in N_j}X_{ik}+\left(\frac{\gamma_i}{\|N_j\|}\sum_{k\in N_j}X_{ik}\right)^2\right)\end{array}\right]}{4\sigma^2\frac{1}{2\beta^2}}}{Z_{ij}\sqrt{2\pi\sigma^2}} \quad (36)$$

and rewritten into Gaussian form;

$$\frac{1}{Z_{ij}\sqrt{2\pi\sigma^2}}\exp\left(\frac{(1+2\frac{1}{2b^2}\sigma^2)}{2\sigma^2}\left[X_{ij}-\frac{(R_{ij}-\mu_i(x_j,y_j)+\frac{2\frac{1}{2\beta^2}\sigma^2\gamma_i}{\|N_j\|}\sum_{k\in N_j}X_{ik})}{(1+2\frac{1}{2\beta^2}\sigma^2)}\right]^2+K(x)\right) \quad (37)$$

where *K(x)* is a parameter constant. From Eq. (37), the means and variance of X_{ij} is shown that;

$$\mu' = \frac{(R_{ij}-\mu_i(x_j,y_j)+\frac{2\frac{1}{2\beta^2}\sigma^2\gamma_i}{\|N_j\|}\sum_{k\in N_j}X_{ik})}{(1+2\frac{1}{2\beta^2}\sigma^2)} \text{ and } \sigma'^2 = \frac{\sigma^2}{(1+2\frac{1}{2\beta^2}\sigma^2)}.$$

From Eq. 32 the derivative is used for finding the maximum point, the chain rule is employed to this Eq..

$$\frac{d}{d(x,y)} = \frac{d}{d\mu(x,y)}\cdot\frac{d\mu(x,y)}{d(x,y)}$$

$$(x_j,y_j)^{opt} = \arg\max_{(x_j,y_j)} log\left[\Pr\left(\boldsymbol{R}_j\middle|(x_j,y_j),\boldsymbol{X}_{iN_j}\right)\right].$$
$$= -\frac{d}{d\mu(x,y)}\frac{(R_{ij}-\mu_i(x_j,y_j)-X_{ij})^2}{2\sigma^2}\cdot\frac{d\mu(x,y)}{d(x,y)} \quad (38)$$

The optimum solution [see in Appendix A] can be obtained by solving

$$\sum_{i=1}^{K}\left\{\frac{10n_{ij}(x_j-a_i)}{(x_j-a_i)^2+(y_j-b_i)^2}\cdot\left(R_{0i}-10n_{ij}log\sqrt{(x_j-a_i)^2+(y_j-b_i)^2}-R_{ij}+\frac{\gamma_i}{\|N_j\|}\cdot\sum_{k\epsilon N_j}X_{ik}\right)\right\}=0 \quad (39)$$

,

and

$$\sum_{i=1}^{K}\left\{\frac{10n_{ij}(y_j-b_i)}{(x_j-a_i)^2+(y_j-b_i)^2}\cdot\left(R_{0i}-10n_{ij}log\sqrt{(x_j-a_i)^2+(y_j-b_i)^2}-R_{ij}+\frac{\gamma_i}{\|N_j\|}\cdot\sum_{k\epsilon N_j}X_{ik}\right)\right\}=0 \quad (40)$$

1.3 The position Estimation of multiple nodes at a time

In this approach, the RSS signal and position of the receiving node are known. However, the location of all transmitting nodes are not known. The objective of this session is find the optimum *(x,y)*.

Let $\boldsymbol{R}=\{R_{ij}|i\in I,j\in J\}$ and$\boldsymbol{X}=\{X_{ij}|i\in I,j\in J\}$ be the set of all RSSs and LD parts of all unknown path loss, the joint probability density function of $\boldsymbol{R}$ and $\boldsymbol{X}$ is given by

$$\Pr(\boldsymbol{R},\boldsymbol{X}|L) = \Pr(\boldsymbol{R}|\boldsymbol{X},L)\Pr(\boldsymbol{X}) \quad (41)$$

where $L=\{(x_1,y_1),\ldots,(x_K,y_K)\}$ is the set of all transmitting node locations. By substituting (25), the above equation becomes

$$\Pr(\boldsymbol{R},\boldsymbol{X}|L) = \frac{1}{Z'}\exp\left[-\sum_{i\in I}\sum_{j\in J}E_{ij}\right] \quad (42)$$

where $E_{ij} = \frac{1}{2\sigma^2}\left(R_{ij} - R_{0j} + 10n_{ij}\log(\frac{d_{ij}}{d_0}) - X_{ij}\right)^2 + \frac{1}{2\beta^2}\left(X_{ij} - \frac{\gamma_i}{\|N_j\|}\sum_{k\in N_j}X_{ik}\right)^2$, and Z' is a normalizing constant. In practice, the direct computation of $Z'$is infeasible since it requires the integration of all possible $\boldsymbol{X}$'s. Hence, we apply the mean field theory (Zhang *et al.*, 1992) to Eq. (42), and the approximated joint PDF is given by

$$\Pr(\boldsymbol{R},\boldsymbol{X}|L) = \prod_{i\in I}\prod_{j\in J}\frac{1}{Z''}\exp\left[-E_{ij}^{avg}\right] \quad (43)$$

where

$$E_{ij}^{avg} = \frac{\left(R_{ij} - R_{0j} + 10n_{ij}\log(\frac{d_{ij}(L)}{d_0}) - X_{ij}\right)^2}{2\sigma^2} + \frac{1}{2\beta^2}\left(X_{ij} - \frac{\gamma_i}{\|N_j\|}\sum_{k\in N_j}E[X_{ik}|L.R]\right)^2,$$

and

$Z'' = 2\pi\sigma\beta.$

where $d_{ij}(L)$ is the distance between transmitting Node *j* and receiving Node *i* when Node j is located at (x_j, y_j), and $E[X_{ik}|L]$ is the expected value of X_{ik}over the *a posteriori* probability of $\boldsymbol{X}_j$ when sensor nodes are located, as specified in *L*. From Bayes' rule and Eq. (43), the *a posteriori* probability of $X_{ij}$is given by

$$\Pr(X_{ik}|\boldsymbol{R},L) = \frac{1}{\sqrt{2\pi\lambda^2}}e^{-\frac{1}{2\lambda^2}\left(X_{ij}-\mu_{ij}(L)\right)^2} \quad (44)$$

where

$$\mu_{ij}(L) = \frac{1}{\lambda^2}\left[{\beta_i}^2\left(-R_{ij} + R_{0j} - 10n_{ij}\log\left(\frac{d_{ij}(L)}{d_0}\right)\right) + {\sigma^2}_i\frac{\gamma_i}{\|N_j\|}\sum_{k\in N_i}E[X_{ik}|L,R]\right],$$

and

$$\lambda^2 = \frac{\sigma^2\beta^2}{\sigma^2+\beta^2}.$$

The locations of all sensor nodes are estimated by using the maximum likelihood estimator (MLE). The MLE is known to provide the minimum estimation error if the estimate is unbiased. In statistics, the MLE is a method of estimating the parameters of a statistical model. The goal is to find L that maximizes the PDF of the observation givens the estimating parameters, i.e.,

$$L^{opt} = \arg\max_{L}\left[\Pr(\boldsymbol{R}_j|L)\right]. \tag{45}$$

Unfortunately, the direct computation of $\Pr(\boldsymbol{R}_j|L)$ is infeasible since it involves the integration of Eq. (42) over all possible LDRPLs form all transmitting nodes. As a result, the expectation maximization (EM) algorithm is employed to iteratively approximate the solution of (45). The EM algorithm is an iterative process composing of two steps, namely expectation (E) and maximization (M) steps. For a given iteration t, the EM algorithm begins with the E-step where the expectation of log-likelihood function of $\Pr(\boldsymbol{R},\boldsymbol{X}|L)$is computed and it is given by

$$\begin{aligned}
&E\left[\log\Pr(\boldsymbol{R},\boldsymbol{X}|L)|\boldsymbol{R},L^{t-1}\right]\\
&= -\frac{1}{2\sigma^2}E\left[\sum_{i\in I}\sum_{j\in J}\left(X_{ij}-\mu_{obv_{ij}}\right)^2\middle|\boldsymbol{R},L^{t-1}\right]\\
&\qquad -\frac{1}{2\beta^2}E\left[\sum_{i\in I}\sum_{j\in J}\left(X_{ij}-\mu_{NG_{ij}}\right)^2\middle|\boldsymbol{R},L^{t-1}\right]+C\\
&= -\frac{1}{2\sigma^2}\sum_{i\in I}\sum_{j\in J}\left(\mu_{ij}(L^{t-1})-\mu_{obv_{ij}}\right)^2-\frac{1}{2\beta^2}\sum_{i\in I}\sum_{j\in J}\left(\mu_{ij}(L^{t-1})-\mu_{NG_{ij}}\right)^2\\
&\qquad +C
\end{aligned} \tag{46}$$

where $\mu_{NG_{ij}} = \frac{\gamma_i}{\|N_j\|}\sum_{k\in N_j}E[X_{ik}]$,$\mu_{obv_{ij}} = -R_{ij}+R_{0j}-10n_{ij}\log\left(\frac{d_{ij}(L)}{d_0}\right)$ and C is constants independent of L.

Next, in M-step, Eq. (46) is maximized with respect to L. The solution can be found by taking derivative of Eq. (46) with respect to sensor node locations and letting the derivative to zero. Hence, the M-step solves for a new set of L by solving

$$\sum_{i \in I} \left(\mu_{ij}(L^{t-1}) - \mu_{obv_{ij}} \right) \frac{\partial \mu_{obv_{ij}}}{\partial x_j} = 0 \tag{47}$$

and

$$\sum_{i \in I} \left(\mu_{ij}(L^{t-1}) - \mu_{obv_{ij}} \right) \frac{\partial \mu_{obv_{ij}}}{\partial y_j} = 0 \tag{48}$$

for all $j \in J$.The E and M-steps are repeated until the solution converges, or the maximum number of iterations is reached. The solution is shown in Appendix A

RESULTS AND DISCUSSION

1. Testing Algorithm in the experiment area

In this research, the RSSI data is collected from the experiment. The sensor nodes used in this experiment are Tmote sky broads with the Chipcon CC2420 wireless transceiver. The experiment is setup in the hall way of the 5th floor Chuchart Kumphu building at Kasetsart University. Figure 5 shows the layout of our experimental set up on the fifth floor.

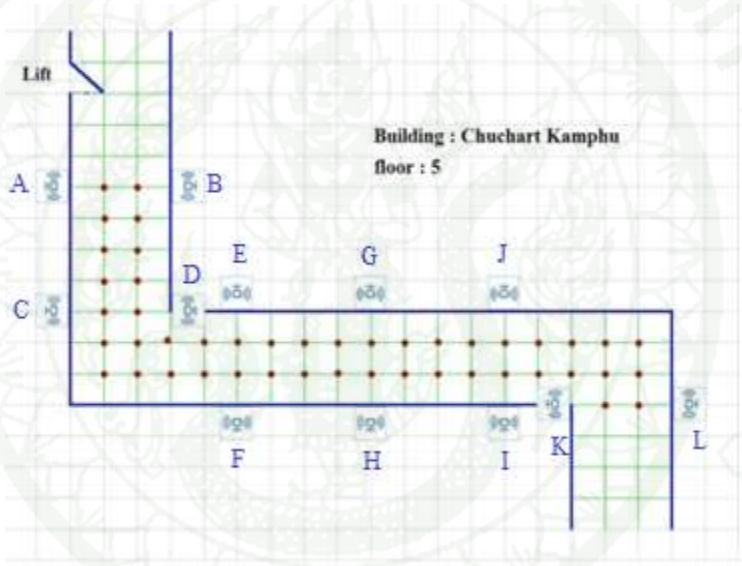

Figure 4 The layout plan showing an experiment area

The ten emitters and the four 4 receivers on the left side of Figure 4 are used to examine the performance of our localization algorithm.

In this test, the blue block is a receiver denoted by symbol *A*, *B*, *C* and *D* receiver node and the 10 circular in area denoting by transmitter nodes (Figure 5). We divide the experiment into two parts. In the first part, we consider the case where a location of a single node (yellow node in Figure 5) is unknown and the rest (red and blue nodes) of the node location are known. In other word, we study the location of neighboring nodes are known. The second part, we investigate the situation where all

transmitting nodes location are unknown, and the algorithm attempts to jointly estimate location of all transmitting nodes.

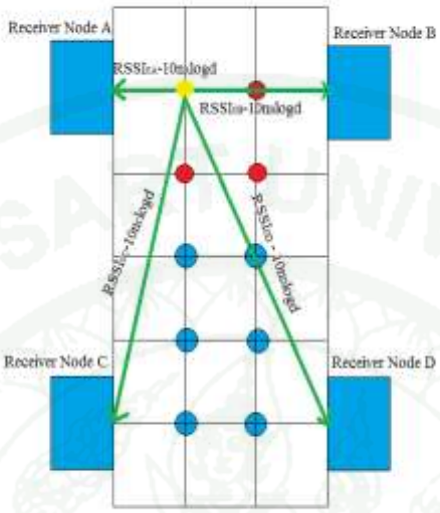

Figure 5 The layout plan showing a first testing algorithm

1.1 Only single node with unknown location

In this experiment, we assume that the receiver node and the neighboring node of the nodes of interest have known position. Here, we rotate each transmitting node to be the node of interest and use the node at the left, right, up, down, up-left, down-left, up-right and down-right of the node of interest as the neighboring nodes. The γ is assumed to depend on each receiver node only. Table 5.1 shows the position of the emitter and compare between position of the emitter, real position and triangulation method. The optimum γ is equal to 0.2616, 0.8039, 0.6654 and 0.14309 for the receiving Nodes A, B, C and D, respectively. Table 5.2 shows the error between position of the emitter, real position and triangulation method.

Table 1 The comparison between actual distance and the estimated location of all transmitter nodes

No. emitter	Method			
	Actual location	**Triangulation**	**single node at a time approach, γ =1**	**single node at a time approach, the optimum γ**
1	(3.32,0)	(2.52, -0.37)	(2.43,0.63)	(2.60,-0.26)
2	(1.66,0)	(2.24,-0.45)	(2.53,0.56)	(2.52,-0.41)
3	(3.32,2)	(2.69,1.36)	(2.75,2.45)	(2.91,2.02)
4	(1.66,2)	(2.82,4.81)	(2.53,3.71)	(2.96,4.36)
5	(3.32,4)	(2.15,3.51)	(1.40,3.56)	(1.92,3.67)
6	(1.66,4)	(2.47,2.41)	(2.64,2.34)	(2.48,2.46)
7	(3.32,6)	(4.12,5.70)	(3.79,6.33)	(3.93,6.27)
8	(1.66,6)	(3.33,6.46)	(3.25,7.37)	(3.25,7.07)
9	(3.32,8)	(2.93,7.22)	(3.36,6.69)	(3.27,7.26)
10	(1.66,8)	(0.85,7.67)	(1.32,8.54)	(1.31,7.95)

Table 2 The RMSE of emitter node in the position estimation of single node at a time approach

	RMSE of distance of all emitter (m)	**Improvement over triangulation approach (cm)**	**Percentage improvement (%)**
Triangulation	1.41775	-	-
Position estimation of single node at a time approach, $\gamma = 1$	1.38526	3.249	2.29%
Position estimation of single node at a time approach, when γ is optimum	1.169972	24.7778	17.48%

1.2 Position Estimation of multiple nodes at a time

In this case, the positions of all emitting nodes are assumed to be unknown. However, a emitting node can determine its neighboring nodes by observed the power of transmitted signal from all nodes. If the power is greater than some predefined value, it will consider these nodes to be its neighboring node. We assume further that the wireless channel is symmetrically, if node *i* make node *k* to be its neighbors, node *k* will also marks node *i* to be the neighbor as well. In the first scenario, we assume that $\gamma_A = \gamma_B = \gamma_C = \gamma_D = \gamma$, and $\sigma_i^2 = \beta_i^2$. In this case, the optimum can be reduce to 1.27208 m

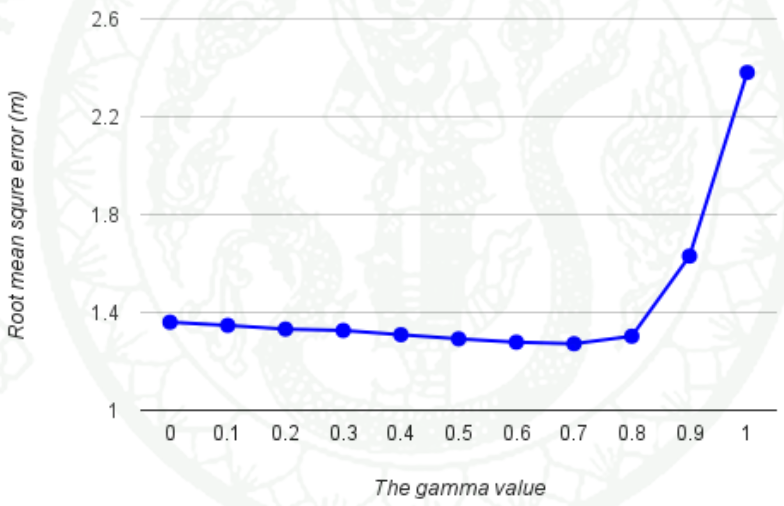

Figure 6 The RMSE of emitter node the position estimation of multiple nodes at a time approach compare between γ =0 and γ =1

We vary the value of γ from 0 to 1 are examine the performance of our algorithm and plot the RMSE versus the value of γ in Fig 6. We observe the value at γ = 0.7 the RMSE is minimal, and the corresponding RMSE equal to 1.27m which is 6.47% less than those of the triangulation approach.

After that we choose the optimum value of γ_A, γ_B, γ_C, γ_D. And the optimum value is $\gamma_A = 0.7735$, $\gamma_B = 0.9648$, $\gamma_C = 0.2883$, $\gamma_D = 0.7178$ for receiver A, B,

C and D respectively. Next, the optimum value of σ_i and β_i are also determine, and their values are given as σ_A = 3.5836, σ_B= 4.2364, σ_C=3.6981, σ_D = 4.1203, b_A = 5.4216, b_B= 6.0307, b_C= 6.3403 and b_D=5.4472. The corresponding performance of the propose localization algorithm is summarized in Table 3. We observe that, the proper parameter selection the RMSE can be reduced as much as 14.10% from the simple triangulation approach. This result confirms our assumption the LDRPL from neighboring nodes are correlated.

Table 3 The RMSE of emitter node in the position estimation of multiple nodes at a time approach

	RMSE of distance of all emitter (m)	**Improvement over triangulation approach (cm)**	**Percentage improvement (%)**
Triangulation	1.36012	-	-
The position estimation of multiple nodes at a time approach, ($\gamma_A = \gamma_B = \gamma_C = \gamma_D$ =γ=0.7)	1.27208	0.08804	6.47%
The position estimation of multiple nodes at a time approach, (optimum values of γ_i)	1.22975	0.13037	9.59%
The position estimation of multiple nodes at a time approach, ($\sigma_i^2 \neq \beta_i^2$)	1.1684	0.19172	14.10%

2. Testing Algorithm in the overall experiment area

After testing algorithm in the small area, we examine our algorithm in the overall experiment area. The area is divided at corner into 3 subareas because the

wireless sensor nodes cannot receive the information from the emitter nodes that are too far. There are three subareas: red, blue and yellow (see Fig.7). In Fig.7, the red area has a 14 emitters and 4 receiver nodes, blue area has 26 emitters and 6 receiver nodes and yellow area has 6 emitters and 2 receiver nodes. In the yellow area the triangulation approach cannot because the triangulation method requires at least three receiver nodes.

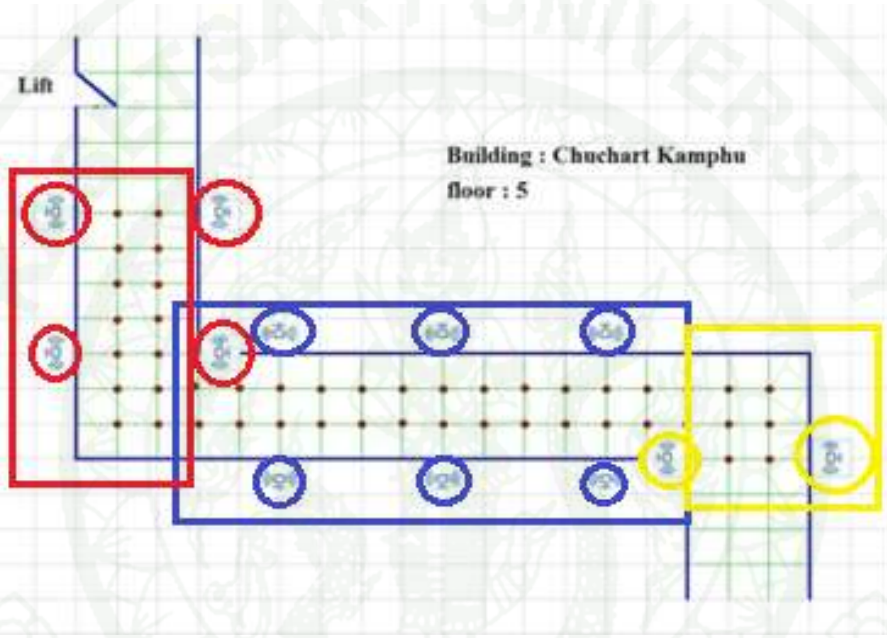

Figure 7 The layout plan showing testing algorithm in the overall experiment area

In this experiment, the triangulation method, the propose algorithm with known position of neighboring nodes and the propose algorithm with unknown position of neighboring nodes are employed for estimation of the transmitting node. The optimum γ of all of receiver nodes are shown in Table 4 for different comparing and corresponding RMSE are summarize the average error is shown in Table 5. The performance of both scenario which position of neighboring nodes are known and unknown are similar, and they are always better than the triangulation method. Furthermore our approach can find the quite accurate location of emitter node where they are only two receiver nodes.

Table 4 The optimum γ in testing algorithm in the overall experiment area

NODE	The position estimation of single node at a time approach	The position estimation of multiple nodes at a time approach
A	0.8605	0.6984
B	0.9377	0.9242
C	0.4462	0.0141
D	0.3227	0.5781
E	0.4568	0.1184
F	0.4667	0.2203
G	0.8235	0.9468
H	0.7681	0.5355
I	0.0142	0.0342
J	1.4288	0.3699
K	1.0106	0.3704
L	1.1143	0.8430

Table 5 The Root Means Square Error comparison between triangulation, the position estimation of single node at a time approach and the position estimation of multiple nodes at a time for testing algorithm in the overall experiment area

Method	RED ZONE			BLUE ZONE			YELLOW ZONE		
	RMSE of distance of all emitter (m)	**Improvement over triangulation approach (m)**	**Percentage improvement (%)**	**RMSE of distance of all emitter (m)**	**Improvement over triangulation approach (m)**	**Percentage improvement (%)**	**RMSE of distance of all emitter (m)**	**Improvement over triangulation approach (m)**	**Percentage improvement (%)**
Triangulation	1.89	-	-	1.86	-	-	N/A	-	-
single node at a time approach ,(γ =1)	1.77	0.11	5.93%	1.85	0.009	0.47%	1.62	-	-
single node at a time approach (optimum γ)	1.59	0.30	15.76%	1.77	0.100	5.26%	1.61	-	-
multiple nodes at a time approach	1.56	0.33	17.30%	1.83	0.038	2.02%	1.84	-	-

The experiment area is the large area with 46 emitter point and 12 receiver nodes. In the first experiment, the area in the left hand side of the fifth floor of Chuchart Kamphu building is used for testing because we want to examine the small scale first. In the result (see Table 2, 3) the package is used in Table 2 and 3 are not equal. In Table 2 we use all of package of data while Table 3 only the six measurement per emitting node due to completely of our propose algorithm for the case of joint position. From the result, it is shown that our algorithm is more accurate than triangulation method. It means that our algorithm can be used for the localization.

Next, our algorithm is examine in the overall testing area for study the feasibility of localization but the overall testing area is very large and the signal in wireless communication is effect by diffraction and reflection when it encounters the corner. The subareas is dived by the corner for avoiding the highly path loss of receiving signal. But the 3rd area or yellow area has a 2 receiver node, the triangulation model doesn't use for calculating the position because the triangulation model can be used if there are at least 3 receiver node. We observe that, the proper parameter selection the RMSE can be reduced as much as 17.30% from the simple triangulation approach in the red area and 5.26% in blue area. Because the scale of the red area is smallest than blue area, the communication effect is lowest than large scale area. This result confirms our assumption the LDRPL from neighboring nodes are correlated.

3. Investigate the node elevation

In this experiment, we will setup new experiment in Chuchart Kamphu floor 5th and use the same Tmote sky as previous. Figure 8 shows the layout of our experimental set up on the fifth floor.

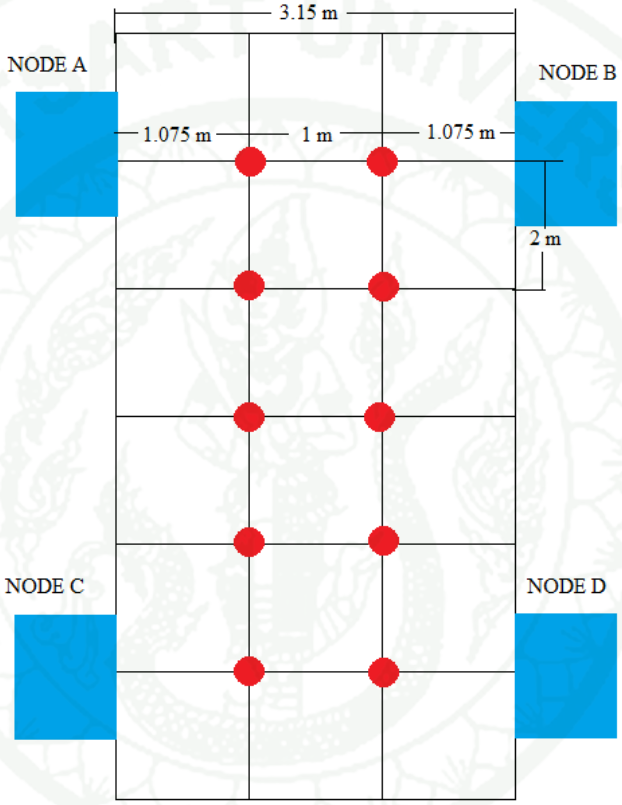

Figure 8 The layout plan showing a new setup experiment area

In the new experiment there are 10 emitter nodes and 4 receiver nodes. The emitting nodes are placed so that they are distanced from the wall, which receiver nodes are placed by 1.075m. The new RSSI data are collected and we divide the experiment into 3 approaches such as emitter node is place on the ground, emitter node is place on the object and emitter node is place on the object and the persons continues walking pass in the experiment area. In the all of case, the effect of the

signal is studied when the antenna of emitter node has change in the different direction (see in Appendix B).

Figure 9 The experiment area

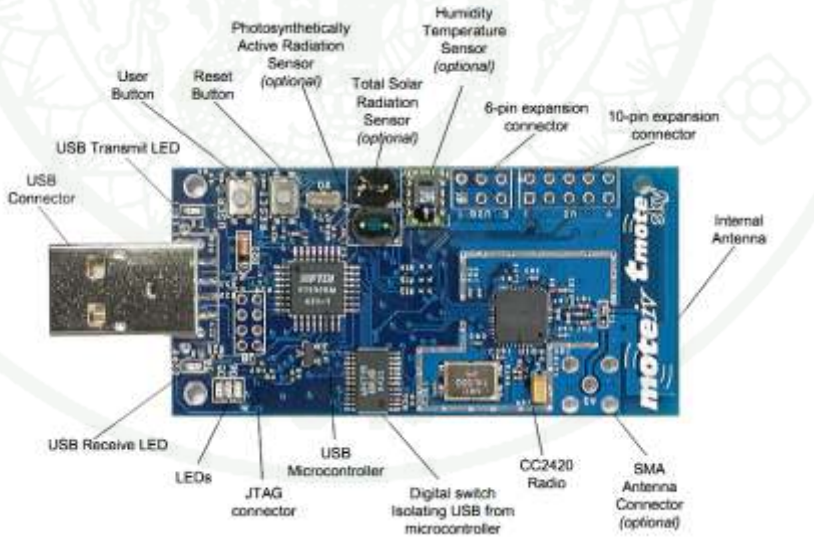

Figure 10 Integrated antenna in Tmote sky (Lorincz, 2006)

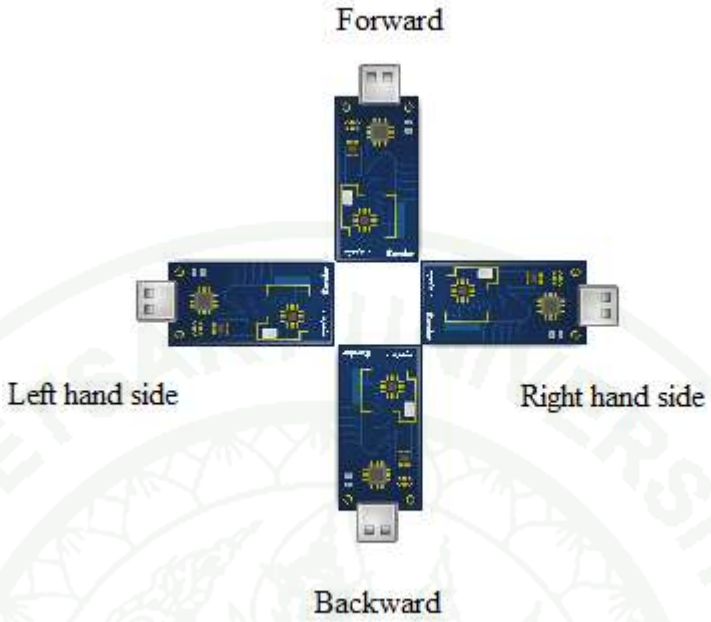

Figure 11 Different direction of Tmote sky

3.1 Emitter node is place on the ground

After testing, we want to study the effect when area has an obstruction such as the table, chair or human etc., the direction of antenna in the emitter node. In the new experiment, we used 10 points of emitter node and 4 receiver node cover in area. In the case 1, the emitter node is placed on the ground and the environment is stationary. The effect by the floor is objective to study. The triangulation method, the position estimation of single node at a time approach and the position estimation of multiple nodes at a time approach are employed to estimating the node positions. The optimum γ of each node is shown in Table 6, the value of $RSSI_0$ and n_{ij} of each receiver node is shown in table 7 and the average error RMSE is shown in table 8.

Table 6 The optimum γ in the case 1

NODE	Right-hand side		Forward		Backward		Left-hand side	
	single node at a time	multiple nodes at a time	single node at a time	multiple nodes at a time	single node at a time	multiple nodes at a time	single node at a time	multiple nodes at a time
A	0.6297	0.5601	0.4120	0.9103	1.3498	0.6309	0.4446	0.9307
B	0.9959	0.9304	0.8560	0.0735	1.4962	1.2892	0.5243	0.1875
C	1.1360	0.5392	1.0266	0.4926	0.6452	0.1625	0.7020	0.8104
D	1.1827	1.0695	1.2080	0.3280	1.7393	0.008	0.2446	1.2828

Table 7 The value of $RSSI_0$ and n_{ij} of each receiver node in the case1

NODE	Right-hand side		Forward		Backward		Left-hand side	
	$RSSI_0$	n_{ij}	$RSSI_0$	n_{ij}	$RSSI_0$	n_{ij}	$RSSI_0$	n_{ij}
A	-42.2477	2.88275	-54.5476	0.847969	-47.7369	2.50382	-39.8795	3.15048
B	-49.4717	2.98979	-48.8302	1.92989	-56.4305	1.73261	-52.2599	2.3746
C	-58.6584	0.713023	-67.1782	0.161113	-58.8361	0.358132	-50.8793	2.23491
D	-43.5685	2.90353	-53.7115	2.14461	-54.4577	1.66489	-51.5857	2.71341

Table 8 The Root Means Square Error comparison between triangulation, the position estimation of single node at a time approach and the position estimation of multiple nodes at a time for testing algorithm in the case 1

Method	Right-hand side			Forward			Backward			Left-hand side		
	RMSE of distance of all emitter (m)	**Improvement over triangulation approach (m)**	**Percentage improvement (%)**	**RMSE of distance of all emitter (m)**	**Improvement over triangulation approach (m)**	**Percentage improvement (%)**	**RMSE of distance of all emitter (m)**	**Improvement over triangulation approach (m)**	**Percentage improvement (%)**	**RMSE of distance of all emitter (m)**	**Improvement over triangulation approach (m)**	**Percentage improvement (%)**
Triangulation	1.22	-	-	2.47	-	-	1.97	-	-	1.25		
single node at a time approach (γ=1)	1.13	0.09	7.07	2.46	0.01	0.59	1.86	0.11	5.41	1.18	0.07	5.77
single node at a time approach γ)	1.09	0.13	10.26	2.40	0.07	2.71	1.49	0.48	24.33	1.15	0.10	7.69
multiple nodes at a time approach	1.11	0.11	8.98	2.41	0.06	2.59	1.86	0.10	5.31	1.17	0.08	6.16

From Table 8, we observe that, the proper parameter selection the RMSE can be reduced as much as 24.33% from the simple triangulation approach in the direction backward. The receive signal is reduced by the reflection, diffraction and interference of the floor. The graph below is shown the RMSE (m) in each direction of all of emitter nodes comparison between all approaches.

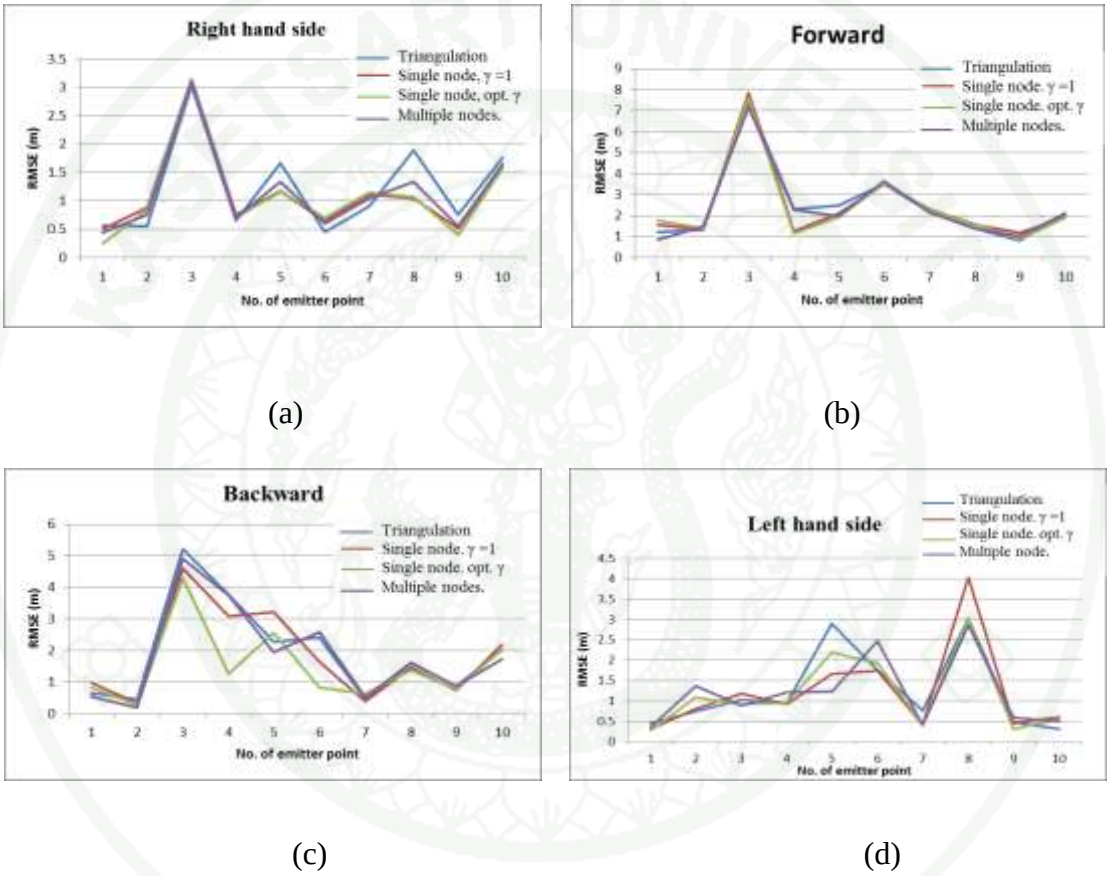

Figure 12 The RMSE (m) of case1 in the direction: (a.) right hand side (b) forward (c.) backward and (d) left hand side compare between all of emitter nodes

From Figure 12, The 3rd node in Figure (a)-(c) has a more error than another point because this point is under the table but Figure (d) has a different trend because in direction left hand side the antenna of emitter node is a direction point leave from the table (see Figure 13).

Figure 13 The position of 3rd node is under the table and direction of antenna when the emitter node has a left hand side direction

3.2 Emitter node is place on the chair

Next, we designed the experiment such that the emitter node is placed on the chair which 1 m height and the environment is a stationary. The triangulation method, the position estimation of single node at a time and the position estimation of multiple nodes at a time are using for estimate the position. The optimum γ of each node is shown in Table 9, the value of $RSSI_0$ and n_{ij} of each receiver node is shown in Table 10 and the average error is shown in Table 11.

Figure 14 Experiment of the case 2

Figure 15 The chair is using in case 2

Table 9 The optimum γ in the case 2

NODE	Right-hand side		Forward		Backward		Left-hand side	
	single node at a time	multiple nodes at a time	single node at a time	multiple nodes at a time	single node at a time	multiple nodes at a time	single node at a time	multiple nodes at a time
A	0.0852	0.7910	0.3345	0.3325	0.0015	0.1471	0.2389	0.7350
B	0.8794	0.3150	0.9050	0.4526	0.4424	0.8293	1.4776	0.9479
C	1.7177	0.7005	0.5127	0.9769	0.8852	1.4496	0.1917	0.7207
D	1.2143	0.8999	0.3869	2.0070	0.9027	0.8531	0.1397	0.9299

Table 10 The value of $RSSI_0$ and n_{ij} of each receiver node in case 2

NODE	Right-hand side		Forward		Backward		Left-hand side	
	$RSSI_0$	n_{ij}	$RSSI_0$	n_{ij}	$RSSI_0$	n_{ij}	$RSSI_0$	n_{ij}
A	-48.8362	1.57307	-47.479	1.94249	-51.8612	1.3042	-49.0837	0.993841
B	-47.9446	1.94507	-47.8151	1.29855	-57.9885	0.839182	-53.5256	0.874594
C	-54.5753	1.13941	-64.3613	-0.2021747	-62.1963	-0.5652338	-59.3546	-0.0131686
D	-54.6884	0.553431	-54.5721	0.890947	-61.7584	-0.4059905	-50.1457	1.41821

Table 11 The Root Means Square Error comparison between triangulation, the position estimation of single node at a time approach and the position estimation of multiple nodes at a time for testing algorithm in the case 2

Method	Right-hand side			Forward			Backward			Left-hand side		
	RMSE of distance of all emitter (m)	**Improvement over triangulation approach (m)**	**Percen-tage improvement (%)**	**RMSE of distance of all emitter (m)**	**Improvement over triangula-tion approach (m)**	**Percen-tage improvement (%)**	**RMSE of distance of all emitter (m)**	**Improvement over triangula-tion approach (m)**	**Percentage improve ment (%)**	**RMSE of distance of all emitter (m)**	**Improvement over triangula-tion approach (m)**	**Percentage improvement (%)**
Triangulation	1.72	-	-	2.05	-	-	2.28	-	-	2.80	-	-
single node at a time (γ=1)	1.69	0.03	1.74	1.88	0.17	8.26	2.00	0.28	12.28	2.66	0.14	5.05
single node at a time (opt. γ)	1.50	0.22	12.79	1.82	0.22	10.90	1.98	0.30	12.30	2.62	0.18	6.59
multiple nodes at a time	1.70	0.02	1.16	1.88	0.17	8.14	2.27	0.01	0.43	2.77	0.04	1.25

From Table 11, the right hand side direction is seem to be the best, the proper parameter selection the RMSE can be reduced as much as 12.79% from the simple triangulation approach. And the graph in Figure 14 shows the RMSE of each emitter nodes for all for sensor nodes orientation.

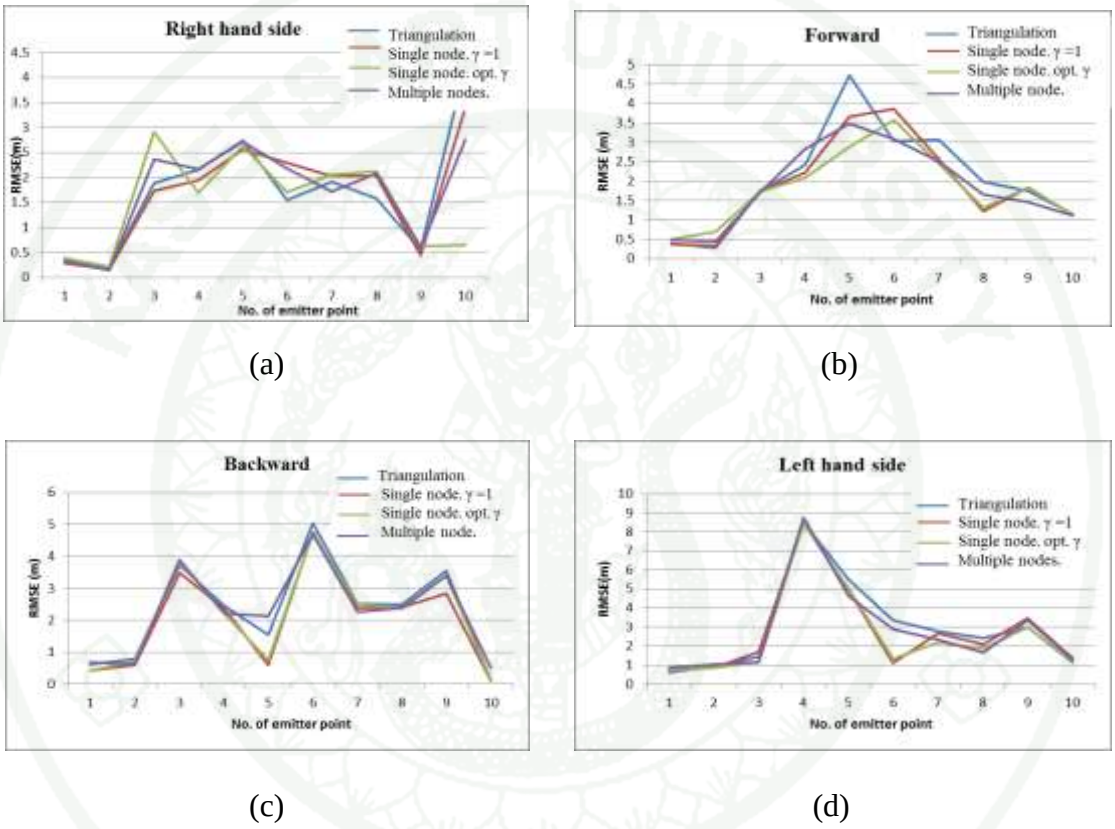

Figure 16 The RMSE (m) of case2 in the direction: (a.) right hand side (b) forward (c.) backward and (d) left hand side compare between all of emitter nodes

From the Figure 16, the trend of the graph on the each direction are vary from one orientation to another. In this case, the path loss exponent of node *C* is negative in direction forward, backward and left hand side. The negative of path loss exponent is mean the receive signal is not reduced by the distance. In our assumption, received signal is attenuated by multipath fading and reduce by the distance and the lognormal model is used for explain the signal in the indoor propagation. Here, the linear regression analysis may not be sufficient.

3.3 Emitter node is place on the object and people walk pass the experiment area.

After that, we will study the effect when the people walk through the experiment area. The environment is the same with case2 (Emitter node is place on the chair) and we design the experiment such that people will be person walk in random path in the experiment area. In this experiment area has a 1 control person and a number of uncontrolled people. The control person walk around the experiment area and walk pass all of receiver node in random path and uncontrolled people walk through the experiment area in random time.

Figure 17 The picture of case 3 with 1 controlled person

Figure 18 The picture of case 3 with 1 controlled person and 1 uncontrolled person

The emitter node is placed on the chair which 1 m height chair and the environment has a people walk through. The triangulation method, the optimum positioning method with known position of neighboring point and the optimum positioning method with unknown position of neighboring point are using for estimate the position. The optimum γ of each node is shown in table 12 and the RMSE is shown in table 13. Because the environment in case 2 and case 3 of experiment is the same except that there is no trespassing person in the area, value of $RSSI_0$ and n_{ij} from case 2 are used in case3.

Table 12 The optimum γ in case 3

NODE	Right-hand side		Forward		Backward		Left-hand side	
	single node at a time	**multiple nodes at a time**	**single node at a time**	**multiple nodes at a time**	**single node at a time**	**multiple nodes at a time**	**single node at a time**	**multiple nodes at a time**
A	0.8456	0.4740	0.7663	0.7111	1.0377	0.1295	0.8942	0.4712
B	0.4109	0.2178	0.5464	0.1107	0.6562	0.0586	1.1493	0.4735
C	1.2600	0.9409	1.2847	0.1539	0.7068	0.5344	1.0188	0.2002
D	0.9918	0.4968	0.0412	1.0019	1.1143	0.0808	1.0251	0.6573

Table 13 The Root Means Square Error comparisons between triangulation, the position estimation of single node at a time approach and the position estimation of multiple nodes at a time for testing algorithm in the case 3

Method	Right-hand side			Forward			Backward			Left-hand side		
	RMSE of distance of all emitter (m)	**Improvement over triangulation approach (m)**	**Percentage improvement (%)**	**RMSE of distance of all emitter (m)**	**Improvement over triangulation approach (m)**	**Percentage improvement (%)**	**RMSE of distance of all emitter (m)**	**Improve ment over triangula-tion approach (m)**	**Percentage improve ment (%)**	**RMSE of distance of all emitter (m)**	**Improvement over triangula-tion approach (m)**	**Percentage improvement (%)**
Triangulation	1.60	-	-	1.98	-	-	2.36	-	-	2.51	-	-
single node at a time (γ=1)	1.58	0.02	1.22%	1.91	0.07	3.48%	2.21	0.16	6.72%	2.21	0.30	12.09%
single node at a time (opt γ)	1.53	0.08	4.89%	1.70	0.28	14.27%	2.17	0.19	8.33%	2.16	0.35	13.96%
multiple nodes at a time	1.52	0.09	5.47%	1.83	0.15	7.56%	2.33	0.03	1.40%	2.32	0.19	7.36%

From Table 13, the forward direction is seem to be the best, the proper parameter selection the RMSE can be reduced as much as 14.27% from the simple triangulation approach. And the graph in Figure 19 shows the RMSE of each emitter nodes for all for sensor nodes orientation.

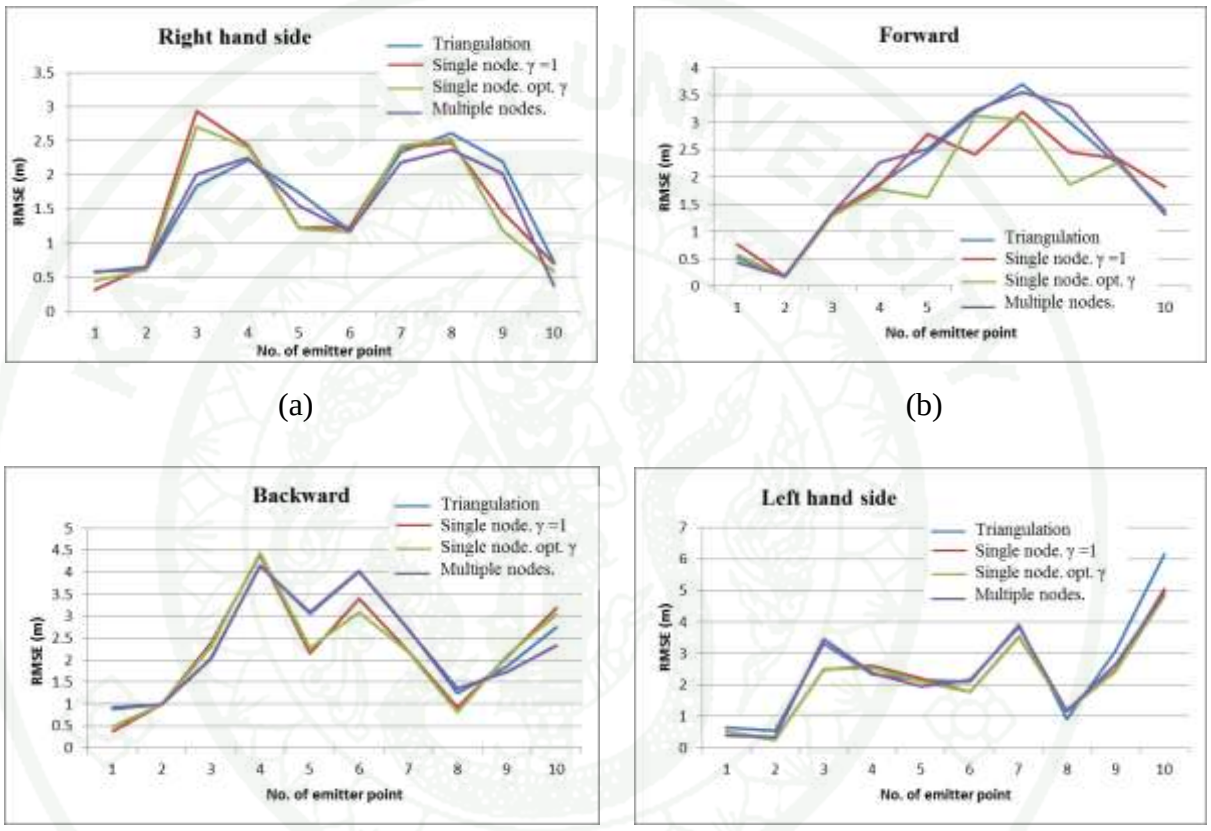

Figure 19 The RMSE (m) of case3 in the direction: (a.) right hand side (b) forward (c.) backward and (d) left hand side compare between all of emitter nodes

From the Figure19, the sensor node is use frequency 2.4 GHz to communicate between them, the human body contains more than 70% water and it is known that resonance frequency of water is 2.4 GHz. Thus the human body reacts as an absorber attenuating the wireless signal but our algorithm can be find the position of emitter node and the root mean square error has a value which is similar to other case. So, we

conclude that the humans can be attenuate the RF signal with little effect. Hence, the performance of case2 and case 3 are similar.

The RMSE of all cases are different. The ANOVA test whether the RMSE from all cases are the same or the different. The ANOVA (Penny *et al*., 2006) or analysis of variance is a flexible method for testing hypotheses about means when there is one independent variable (IV), with two or more levels, and one dependent variable (DV). The probability value which find from ANOVA is used to analysis the similar of average error. The p-value is 0.876358542; it shows that the RMSE of all cases are similar.

CONCLUSION AND RECOMMENDATIONS

Conclusion

From the experimental result, the position which find from the position estimation of single node at a time approach and the position estimation of multiple nodes at a time approach are more accurate than triangulation method in all of cases. The different environments have effect with the accuracy. In this work, the cooperative localization algorithm is proposed. Here, the sensor network combines the RSS values for neighboring sensors by using the MRF model. Our numerical result shows that, with the proper selection of the parameter, the accuracy can be significantly improved.

The computational tool is significant in this research because it used for finding the position of the emitter node. The linear regression analysis approach is the one which choose because it is simple and make the signal model to be relative with assumption. Hence, linear regression analysis may not be sufficient; the some cases are not relative with our assumption. Likewise, the Matlab is the software computational tool which is known and worldwide. It used for find the solution of our equation but we haven't seen method which the program is used for find the solution, this point that we want to find the method and analyze that method is proposed for our equation.

The same environment in the different day assumes to be the same and experimental area is an open air. The uncontrollable parameters such as wifi hotspot wind etc. affect signal in the wireless channel. These parameters may be make differential experiment in the different day but we assume all experiment to be same. The result is shown that the difference between cases, the ANOVA is shown similar of all cases. The ANOVA shown that the RMSE of all case is similar due to 88% so we conclude that the dynamics environment and the static environment have a similar affect in the wireless channel.

Recommendation

Our algorithm is used for statistically wireless sensor network, the emitter node isn't movement and the data will be collected by 1 emitter node. In the future, the experiment will be setup with movement emitter node and study the affect when the high of the chair will be placed, are change. Then we want to experiment about number of receiver node is more than this experiment and study the effect in this experimental area.

The computational tool is will be change because we think that our tools make the signal model which is not relative with our assumption in the some cases. The experiment area will be the close because it is easy to find the reason when the position of emitter node has a more error.

LITERATURE CITED

Anindya, S. P. October 2009. RSSI-Based Indoor Localization and Tracking Using Sigma-Point Kalman Smoothers. **IEEE journal of selected topics in signal processing,** 3(5):860-73.

Borman, S. January 2009. **The Expectation Maximization Alogorithm**.

Cottrell, A. 2003. **Regression Analysis: Basic Concepts**.

Guoqiang M., B. Fidan and D.O. Anderson. 2006. **Wireless Sensor Network Localization Techniques.**

Kasetkasem, T. 2002. **Image Analysis Method based on Markov Random Fields**. Ph.D. Thesis, Syracuse University.

Kline, P. A. 1997**. Atomic Clock Augmentation For Receivers Using the Global Positioning System**. 28-49.

Lorincz, K. 2006. **Project shimmer reference Tmote sky Datasheet**, Harvard University. Available source: http://www.eecs.harvard.edu/~konrad/projects/shimmer/references/tmote-sky-datasheet.pdf

Myung, J. 2003. Tutorial on maximum likelihood estimation. **Journal of Mathematical Psychology.** 47: 90–100.

Parameswaran, A. T., M. I. Husain and S. Upadhyaya. 2009. **Is RSSI a Reliable Parameter in Sensor Localization Algorithms – An Experimental Study. – An Experimental Study.** Field Failure Data Analysis Workshop (F2DA,09). New York USA,.

Penny, W. and R. Henson. May 2006. **Chapter 13: Analysis of Variance**.

Potiban, L. 2010. **562701 The Design and Research of Nurse and Analysis**, Chaingmai University course work. 283-323.

Ray, A., D. Starobinski, A. Trachtenberg and R. Ungrangsi. 2004. Robust Location Detection with Sensor Networks. **IEEE Journal on Selected Areas in Communications**. 22(6): 1016-25.

Rong, P. and M. L. Sichitiu. 2006. **Angle of Arrival Localization for Wireless Sensor Networks**.

Stankovic, J.A. 2006. **Wireless Sensor Networks.** University of Virginia**,** 1-8**.**

Sundaresan, A. and P. K. Varshney. February 2011. Location Estimation of a Random Signal Source Based on Correlated Sensor Observations. **IEEE transection on signal processing,** 59 (2): 787-99.

Taylor, E. F. 2003. **Global Positioning System.**

Winkler, G. 2003. **Image Analysis,Random Field and Dynamics Monte Carlo Methods**, Springer Berlin Heidelberg New York, :159-177

Zhang, J. October 1992. The mean field theory in EM procedures for Markov random fields, **Signal Processing, IEEE Transactions on,** 40(10): 2570-83.

Zhang, J and L. Zhang. 2009. Research on Distance Measurement Based on RSSI of ZigBee. **ISECS International Colloquium on Computing, Communication, Control, and Management. IEEE.**

APPENDICES

APPENDIX A

Solution of equation

1. The position estimation of single node at a time

Represent $\frac{1}{2\beta^2}$ by β

$$(x_j,y_j)^{opt} = \arg\max_{(x_j,y_j)} log\left[\Pr\left(\boldsymbol{R}_j\middle|(x_j,y_j),\boldsymbol{X}_{iN_j}\right)\right].$$

$$0 = -\frac{d}{d\mu(x,y)}\frac{(R_{ij}-\mu_i(x_j,y_j)-X_{ij})^2}{2\sigma^2}\cdot\frac{d\mu(x,y)}{d(x,y)} \quad (1)$$

$$\frac{d\mu(x,y)}{d(x)} = -\frac{10n_{ij}(x_j-a_i)}{(x_j-a_i)^2+(y_j-b_i)^2} \quad (2)$$

and,

$$\frac{d\mu(x,y)}{d(y)} = -\frac{10n_{ij}(y_j-b_i)}{(x_j-a_i)^2+(y_j-b_i)^2} \quad (3)$$

Then,

$$\frac{d}{d\mu(x,y)}\frac{(R_{ij}-\mu_i(x_j,y_j)-X_{ij})^2}{2\sigma^2}$$
$$= \frac{d}{d\mu(x,y)}\frac{(R_{ij}{}^2-2\mu_i(x_j,y_j)R_{ij}-2R_{ij}X_{ij}+\mu_i(x_j,y_j)^2+2\mu_i(x_j,y_j)X_{ij}+X_{ij}{}^2)}{2\sigma^2} \quad (4)$$

When mean and variance of random path loss is:

$\mu' = \frac{(R_{ij}-\mu_i(x_j,y_j)+\frac{2\beta\sigma^2\gamma_i}{\|N_j\|}\Sigma_{k\in N_j}X_{ik})}{(1+2\beta\sigma^2)}$ and $\sigma'^2 = \frac{\sigma^2}{(1+2\beta\sigma^2)}$.

X_{ij} is represent by μ' and $X_{ij}{}^2$ is represent by $\sigma^2+\mu_i{}'^2$

$$= \frac{d}{d\mu(x,y)}\frac{(R_{ij}{}^2-2\mu_i(x_j,y_j)R_{ij}-2R_{ij}\mu_i{}'+\mu_i(x_j,y_j)^2+2\mu_i(x_j,y_j)\mu_i{}'+\sigma^2+\mu_i{}'^2)}{2\sigma^2} \quad (5)$$

$$= \frac{d}{d\mu(x,y)}\frac{(-2\mu_i(x_j,y_j)R_{ij}-2R_{ij}\mu_i{}'+\mu_i(x_j,y_j)^2+2\mu_i(x_j,y_j)\mu_i{}'+\mu_i{}'^2)}{2\sigma^2} \quad (6)$$

When

$$\frac{d\mu_i{}'}{d\mu(x,y)} = \frac{d}{d\mu(x,y)}\frac{(R_{ij}-\mu_i(x_j,y_j)+\frac{2\beta\sigma^2\gamma_i}{\|N_j\|}\Sigma_{k\in N_j}X_{ik})}{(1+2\beta\sigma^2)} = -\frac{1}{(1+2\beta\sigma^2)} \quad (7)$$

$$\frac{d(2\mu_i(x_j,y_j)\mu_i{}')}{d\mu(x,y)} = 2\left(\left[\mu_i(x_j,y_j)\cdot -\frac{1}{(1+2\beta\sigma^2)}\right] + \mu_i{}'\right) \quad (8)$$

$$\frac{d\mu_i{}'^2}{d\mu(x,y)} = 2\mu_i{}'\cdot -\frac{1}{(1+2\beta\sigma^2)} = -2\left[\frac{(R_{ij}-\mu_i(x_j,y_j)+\frac{2\beta\sigma^2\gamma_i}{\|N_j\|}\sum_{k\in N_j}X_{ik})}{(1+2\beta\sigma^2)^2}\right] \quad (9)$$

$$= -\frac{2R_{ij}}{2\sigma^2} + \frac{2R_{ij}}{2\sigma^2(1+2\beta\sigma^2)} + \frac{2\mu_i(x_j,y_j)}{2\sigma^2} - \frac{2\mu_i(x_j,y_j)}{2\sigma^2(1+2\beta\sigma^2)} + \frac{2\mu_i{}'}{2\sigma^2}$$
$$- \frac{2R_{ij}}{2\sigma^2(1+2\beta\sigma^2)^2} + \frac{2\mu_i(x_j,y_j)}{2\sigma^2(1+2\beta\sigma^2)^2} - \frac{4\sigma^2\beta\frac{\gamma_i}{\|N_j\|}\sum_{k\in N_j}X_{ik}}{2\sigma^2(1+2\beta\sigma^2)^2} \quad (10)$$

So,

$$= \frac{1}{2\sigma^2(1+2\beta\sigma^2)^2}\left(\begin{aligned} &-2R_{ij}(1+2\beta\sigma^2)^2 + 2R_{ij}(1+2\beta\sigma^2) \\ &+ 2\mu_i(x_j,y_j)(1+2\beta\sigma^2)^2 - 2\mu_i(x_j,y_j)(1+2\beta\sigma^2) \\ &+ 2\mu_i{}'(1+2\beta\sigma^2)^2 - 2R_{ij} + 2\mu_i(x_j,y_j) - 4\sigma^2\beta\frac{\gamma_i}{\|N_j\|}\sum_{k\in N_j}X_{ik}\end{aligned}\right) \quad (11)$$

$$= \frac{1}{2\sigma^2(1+2\beta\sigma^2)^2}\left(\begin{aligned} &-2R_{ij}(1+2\beta\sigma^2)^2 + 2R_{ij}(1+2\beta\sigma^2) \\ &+ 2\mu_i(x_j,y_j)(1+2\beta\sigma^2)^2 - 2\mu_i(x_j,y_j)(1+2\beta\sigma^2) \\ &+ 2\frac{(R_{ij}-\mu_i(x_j,y_j)+\frac{2\beta\sigma^2\gamma_i}{\|N_j\|}\sum_{k\in N_j}X_{ik})}{(1+2\beta\sigma^2)}(1+2\beta\sigma^2)^2 - 2R_{ij} \\ &+ 2\mu_i(x_j,y_j) - 4\sigma^2\beta\frac{\gamma_i}{\|N_j\|}\sum_{k\in N_j}X_{ik}\end{aligned}\right) \quad (12)$$

$$= \frac{1}{2\sigma^2(1+2\beta\sigma^2)^2}\Bigg(-2R_{ij}(1+2\beta\sigma^2)^2 + 2R_{ij}(1+2\beta\sigma^2) + 2\mu_i(x_j,y_j)(1+2\beta\sigma^2)^2 - 2\mu_i(x_j,y_j)(1+2\beta\sigma^2) + 2R_{ij}(1+2\beta\sigma^2) - 2\mu_i(x_j,y_j)(1+2\beta\sigma^2) + \frac{4\beta\sigma^2\gamma_i}{\|N_j\|}\sum_{k\in N_j} X_{ik}(1+2\beta\sigma^2) - 2R_{ij} + 2\mu_i(x_j,y_j) - 4\sigma^2\beta\frac{\gamma_i}{\|N_j\|}\sum_{k\in N_j} X_{ik}\Bigg) \quad (13)$$

$$= \frac{1}{2\sigma^2(1+2\beta\sigma^2)^2}\Bigg(-2R_{ij}(1+2\beta\sigma^2)^2 + 4R_{ij}(1+2\beta\sigma^2) + 2\mu_i(x_j,y_j)(1+2\beta\sigma^2)^2 - 4\mu_i(x_j,y_j)(1+2\beta\sigma^2) + \frac{4\beta\sigma^2\gamma_i}{\|N_j\|}\sum_{k\in N_j} X_{ik}(1+2\beta\sigma^2) - 2R_{ij} + 2\mu_i(x_j,y_j) - 4\sigma^2\beta\frac{\gamma_i}{\|N_j\|}\sum_{k\in N_j} X_{ik}\Bigg) \quad (14)$$

$$= \frac{1}{2\sigma^2(1+2\beta\sigma^2)^2}\Bigg(-2R_{ij}[(1+2\beta\sigma^2)^2 - 2(1+2\beta\sigma^2) + 1] + 2\mu_i(x_j,y_j)[(1+2\beta\sigma^2)^2 - 2(1+2\beta\sigma^2) + 1] + \frac{4\beta\sigma^2\gamma_i}{\|N_j\|}\sum_{k\in N_j} X_{ik}[(1+2\beta\sigma^2) - 1]\Bigg) \quad (15)$$

$$= \frac{1}{2\sigma^2(1+2\beta\sigma^2)^2}\Bigg(-2R_{ij}[(1+2\beta\sigma^2) - 1]^2 + 2\mu_i(x_j,y_j)[(1+2\beta\sigma^2) - 1]^2 + \frac{4\beta\sigma^2\gamma_i}{\|N_j\|}\sum_{k\in N_j} X_{ik}[(1+2\beta\sigma^2) - 1]\Bigg) \quad (16)$$

$$= \frac{(1+2\beta\sigma^2) - 1}{2\sigma^2(1+2\beta\sigma^2)^2}\Bigg(-2R_{ij}[2\beta\sigma^2] + 2\mu_i(x_j,y_j)[2\beta\sigma^2] + \frac{4\beta\sigma^2\gamma_i}{\|N_j\|}\sum_{k\in N_j} X_{ik}\Bigg) \quad (17)$$

$$= \frac{(2\beta\sigma^2)(4\beta\sigma^2)}{2\sigma^2(1+2\beta\sigma^2)^2}\left(-R_{ij} + \mu_i(x_j, y_j) + \frac{\gamma_i}{\|N_j\|}\sum_{k\in N_j} X_{ik}\right) \quad (18)$$

From,

$$0 = -\frac{d}{d\mu(x,y)}\frac{(R_{ij} - \mu_i(x_j, y_j) - X_{ij})^2}{2\sigma^2}\cdot\frac{d\mu(x,y)}{d(x,y)}$$

$$0 = \frac{(2\beta\sigma^2)(4\beta\sigma^2)}{2\sigma^2(1+2\beta\sigma^2)^2}\left(-R_{ij} + \mu_i(x_j, y_j) + \frac{\gamma_i}{\|N_j\|}\sum_{k\in N_j} X_{ik}\right) \cdot \frac{10n_{ij}(x_j - a_i)}{(x_j - a_i)^2 + (y_j - b_i)^2} \quad (19)$$

$$0 = \left(-R_{ij} + R_{0i} - 10n_{ij}\log\sqrt{(x_j - a_i)^2 + (y_j - b_i)^2} - R_{ij} + \frac{\gamma_i}{\|N_j\|}\sum_{k\in N_j} X_{ik}\right) \cdot \frac{10n_{ij}(x_j - a_i)}{(x_j - a_i)^2 + (y_j - b_i)^2} \quad (19)$$

$$\sum_{i=1}^{K}\left\{\frac{10n_{ij}(x_j - a_i)}{(x_j - a_i)^2 + (y_j - b_i)^2}\cdot\left(R_{0i} - 10n_{ij}\log\sqrt{(x_j - a_i)^2 + (y_j - b_i)^2} - R_{ij} + \frac{\gamma_i}{\|N_j\|}\cdot \sum_{k\in N_j} X_{ik}\right)\right\} = 0 \quad (20)$$

$$\sum_{i=1}^{K}\left\{\frac{10n_{ij}(y_j - b_i)}{(x_j - a_i)^2 + (y_j - b_i)^2}\cdot\left(R_{0i} - 10n_{ij}\log\sqrt{(x_j - a_i)^2 + (y_j - b_i)^2} - R_{ij} + \frac{\gamma_i}{\|N_j\|}\cdot \sum_{k\in N_j} X_{ik}\right)\right\} = 0 \quad (21)$$

$\frac{d\mu(x,y)}{d(x)}$ can be computed in the similar way.

2. The position estimation of multiple nodes at a time

$$\sum_{i\in I}\left(\mu_{ij}(L^{t-1}) - \mu_{obv_{ij}}\right)\frac{\partial\mu_{obv_{ij}}}{\partial x_j} = 0 \quad (22)$$

and

$$\sum_{i\epsilon I}\left(\mu_{ij}(L^{t-1})-\mu_{obv_{ij}}\right)\frac{\partial\mu_{obv_{ij}}}{\partial y_j}=0 \qquad (23)$$

From (1) ;

When

$\mu_{ij}(L)=\frac{1}{\lambda^2}\left[\beta^2\left(-R_{ij}+R_{0j}-10n_{ij}\log\left(\frac{d_{ij}(L)}{d_0}\right)\right)+\sigma^2\frac{\gamma_i}{\|N_j\|}\sum_{k\epsilon N_j}E[X_{ik}|L]\right]$ and

$\mu_{obv_{ij}}=-R_{ij}+R_{0j}-10n_{ij}\log\left(\frac{d_{ij}(L)}{d_0}\right)$

The solution is:

$$\sum_{i\epsilon I}\left(\frac{1}{\lambda^2}\left[\beta^2\left(-R_{ij}+R_{0j}-10n_{ij}\log\left(\frac{d_{ij}(L)}{d_0}\right)\right)+\sigma^2\frac{\gamma_i}{\|N_j\|}\sum_{k\epsilon N_j}E[X_{ik}|L]\right]-\left(-R_{ij}+R_{0j}-10n_{ij}\log\left(\frac{d_{ij}(L)}{d_0}\right)\right)\cdot\frac{10n_{ij}(x_j-a_i)}{(x_j-a_i)^2+(y_j-b_i)^2}=0 \qquad (24)$$

$$\sum_{i\epsilon I}\left(\left[\frac{\beta^2}{\lambda^2}\left(-R_{ij}+R_{0j}-10n_{ij}\log\left(\frac{d_{ij}(L)}{d_0}\right)\right)+\frac{\sigma^2}{\lambda^2}\frac{\gamma_i}{\|N_j\|}\sum_{k\epsilon N_j}E[X_{ik}|L]\right]-\left(-R_{ij}+R_{0j}-10n_{ij}\log\left(\frac{d_{ij}(L)}{d_0}\right)\right)\cdot\frac{10n_{ij}(x_j-a_i)}{(x_j-a_i)^2+(y_j-b_i)^2}=0 \qquad (25)$$

$$\sum_{i\epsilon I}\left[\left(\frac{\beta^2}{\lambda^2}-1\right)\cdot\left(-R_{ij}+R_{0j}-10n_{ij}\log\left(\frac{d_{ij}(L)}{d_0}\right)\right)+\frac{\sigma^2}{\lambda^2}\frac{\gamma_i}{\|N_j\|}\sum_{k\epsilon N_j}E[X_{ik}|L]\right]\cdot\frac{10n_{ij}(x_j-a_i)}{(x_j-a_i)^2+(y_j-b_i)^2}=0 \qquad (26)$$

$$\sum_{i\epsilon I}\frac{1}{\lambda^2}\left[(\beta^2-\lambda^2)\cdot\left(-R_{ij}+R_{0j}-10n_{ij}\log\left(\frac{d_{ij}(L)}{d_0}\right)\right)+\sigma^2\frac{\gamma_i}{\|N_j\|}\sum_{k\epsilon N_j}E[X_{ik}|L]\right]\cdot\frac{10n_{ij}(x_j-a_i)}{(x_j-a_i)^2+(y_j-b_i)^2}=0 \qquad (27)$$

When $\lambda^2=\frac{\sigma^2\beta^2}{\sigma^2+\beta^2}$

$$\sum_{i\epsilon I}\frac{\sigma^2+\beta^2}{\sigma^2\beta^2}\left[(\beta^2-\frac{\sigma^2\beta^2}{\sigma^2+\beta^2})\cdot\left(-R_{ij}+R_{0j}-10n_{ij}\log\left(\frac{d_{ij}(L)}{d_0}\right)\right)+\sigma^2\frac{\gamma_i}{\|N_j\|}\sum_{k\epsilon N_j}E[X_{ik}|L]\right]\cdot\frac{10n_{ij}(x_j-a_i)}{(x_j-a_i)^2+(y_j-b_i)^2}=0 \qquad (28)$$

$$\sum_{i\epsilon I}\frac{\sigma^2+\beta^2}{\sigma^2\beta^2}\left[\left(\frac{\sigma^2\beta^2+\beta^4-\beta^2\sigma^2}{\sigma^2+\beta^2}\right)\cdot\left(-R_{ij}+R_{0j}-10n_{ij}\log\left(\frac{d_{ij}(L)}{d_0}\right)\right)+\sigma^2\frac{\gamma_i}{\|N_j\|}\sum_{k\in N_j}E[X_{ik}|L]\right]\cdot\frac{10n_{ij}(x_j-a_i)}{(x_j-a_i)^2+(y_j-b_i)^2}=0 \quad (29)$$

$$\sum_{i\epsilon I}\frac{\sigma^2+\beta^2}{\sigma^2\beta^2}\left[\left(\frac{\beta^4}{\sigma^2+\beta^2}\right)\cdot\left(-R_{ij}+R_{0j}-10n_{ij}\log\left(\frac{d_{ij}(L)}{d_0}\right)\right)+\sigma^2\frac{\sigma^2+\beta^2}{\sigma^2+\beta^2}\frac{\gamma_i}{\|N_j\|}\sum_{k\in N_j}E[X_{ik}|L]\right]\cdot\frac{10n_{ij}(x_j-a_i)}{(x_j-a_i)^2+(y_j-b_i)^2}=0 \quad (30)$$

$$\sum_{i\epsilon I}\frac{1}{\sigma^2\beta^2}\left[\beta^4\cdot\left(-R_{ij}+R_{0j}-10n_{ij}\log\left(\frac{d_{ij}(L)}{d_0}\right)\right)+(\sigma^4+\sigma^2\beta^2)\cdot\frac{\gamma_i}{\|N_j\|}\sum_{k\in N_j}E[X_{ik}|L]\right]\cdot\frac{10n_{ij}(x_j-a_i)}{(x_j-a_i)^2+(y_j-b_i)^2}=0 \quad (31)$$

When $\sigma^2=\beta^2$

$$\sum_{i\epsilon I}\frac{1}{\beta^4}\left[\beta^4\cdot\left(-R_{ij}+R_{0j}-10n_{ij}\log\left(\frac{d_{ij}(L)}{d_0}\right)\right)+(2\beta^4)\cdot\frac{\gamma_i}{\|N_j\|}\sum_{k\in N_j}E[X_{ik}|L]\right]\cdot\frac{10n_{ij}(x_j-a_i)}{(x_j-a_i)^2+(y_j-b_i)^2}=0 \quad (32)$$

$$\sum_{i\epsilon I}\left[\left(-R_{ij}+R_{0j}-10n_{ij}\log\left(\frac{d_{ij}(L)}{d_0}\right)\right)+\frac{2\gamma_i}{\|N_j\|}\sum_{k\in N_j}E[X_{ik}|L]\right]\cdot\frac{10n_{ij}(x_j-a_i)}{(x_j-a_i)^2+(y_j-b_i)^2}=0 \quad (33)$$

Equation (23) can be computed in the similar way.

APPENDIX B

Experimental Setup

1. Setup new experiment

1.1 Experiment area

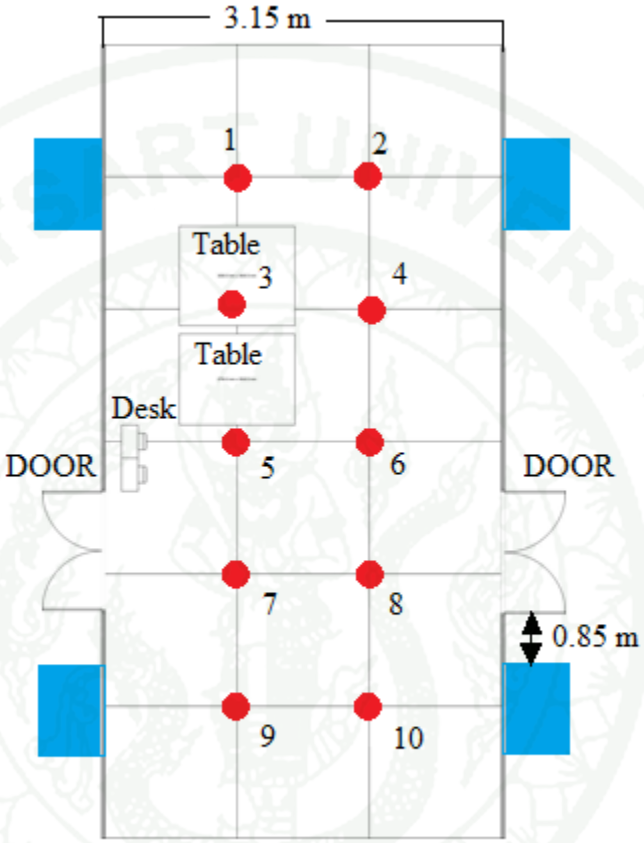

Appendix Figure B1 Floor plan area

The experiment area is 3.15 x 8 m^2 and RSSI data are collected by using Tmote sky node which put on the red point and the receiver nodes are put on the wall and shown in the red circle in Figure AppendixB2.

Appendix Figure B2 position of receiver nodes

Appendix Figure B3 receiver node

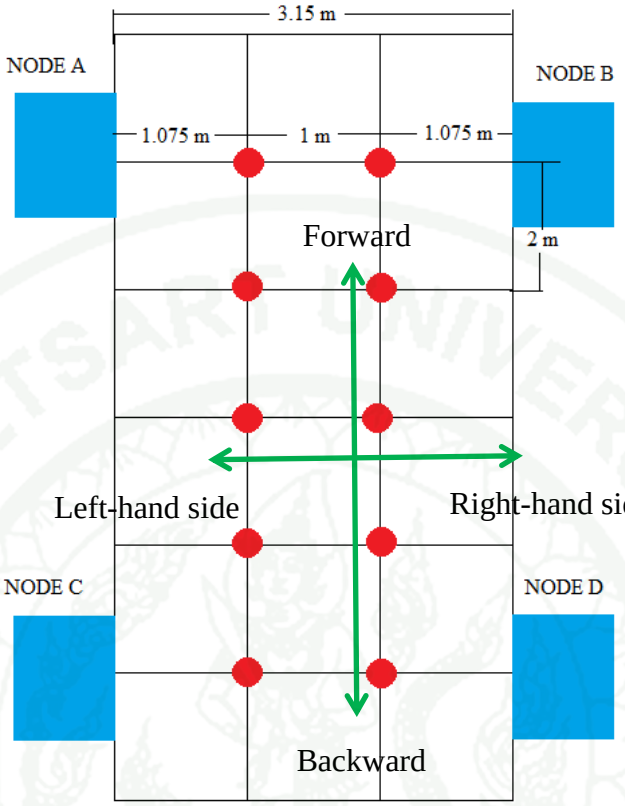

Appendix Figure B4 direction use for transmitter node

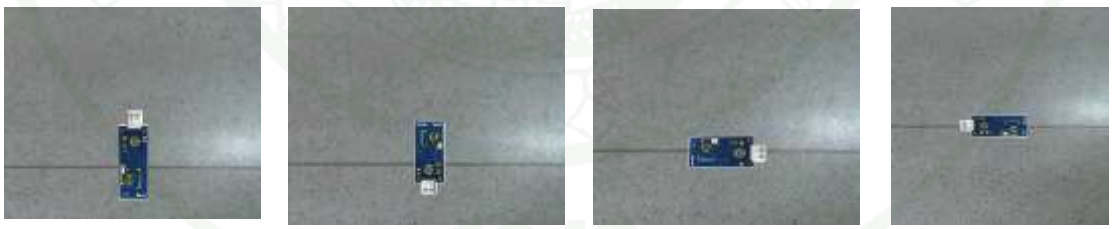

(a) (b) (c) (d)

Appendix Figure B5 Transmitter node in different direction: (a) Forward (b) Backward (c) Right –hand side (d) Left-hand side

Appendix Figure B6 The sensor node which is receive data from the receiver node

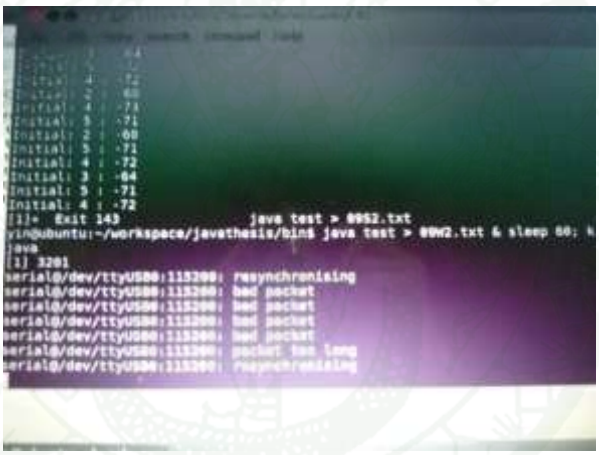

Appendix Figure B7 receiving data

Appendix Figure B8 The red circle is shown the table which computer is placed and experiment area start from first column in the green frame ≈6 m

2. The experimental

Appendix Figure B9 case 2 experiment

In the case 2 experiment, the object is 1 m height and has not a movement object inside experiment area.

In the case 3 experiment, the environment is the same as case 2 and has a people walk passed the experiment area in the random time. In this experiment area

has a 1 control person and uncontrolled people. The control person walk around the experiment area and walk pass all of receiver node in random path and uncontrolled people walk through the experiment area in random time.

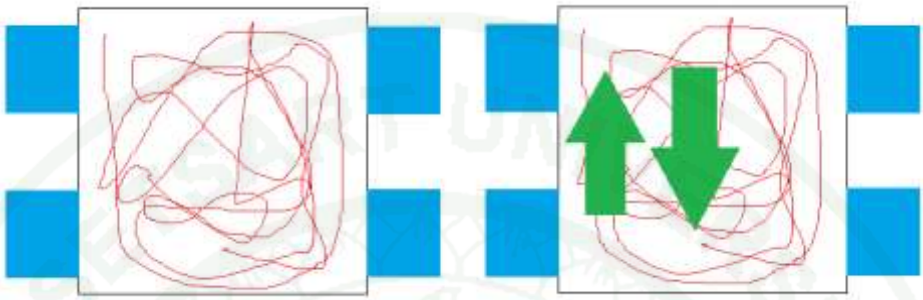

(a) (b)

Appendix Figure B10 a) the example path of 1 controlled person (b) the green arrow is shown the uncontrolled people walk in the direction forward and backward

Appendix Figure B11 The example random path of 1 controlled person

Appendix Figure B12 The example path of the people in the experiment area

APPENDIX C

Positioning result

1. The positioning result

Appendix Table C1 The case1 right-hand side positioning result

No. emitter	Position				
	Actual distance	**Triangulation**	**single node at a time,γ =1**	**single node at a time, the optimum γ**	**multiple nodes at a time**
1	(1.075,0)	(1.62,0.94)	(2.27,0.96)	(2.35,1.15)	(1.29,0.7)
2	(2.075,0)	(2.22,-0.12)	(2.50,-0.43)	(2.51,-0.46)	(2.16,-0.37)
3	(1.075,2)	(3.90,8.71)	(3.60,9.33)	(3.55,9.09)	(3.16,8.52)
4	(2.075,2)	(2.21,2.62)	(2.79,2.33)	(2.70,1.80)	(2.09,2.57)
5	(1.075,4)	(3.22,2.78)	(2.85,2.89)	(2.59,2.80)	(2.37,2.59)
6	(2.075,4)	(2.96,0.97)	(2.64,0.90)	(2.63,0.85)	(3.05,0.91)
7	(1.075,6)	(3.23,6.20)	(3.31,6.53)	(3.27,6.57)	(3.19,6.19)
8	(2.075,6)	(3.03,7.00)	(3.06, 7.21)	(3.07,7.24)	(3.04,7.00)
9	(1.075,8)	(1.84,7.85)	(1.80,7.06)	(1.58,7.30)	(1.99,8.26)
10	(2.075,8)	(0.02,7.66)	(0.17,7.88)	(0.16,7.90)	(0.00055,7.67)

Table AppendixC2 The case1 forward positioning result

No.	Position				
No. emitter	Actual distance	Triangulation	single node at a time,γ =1	single node at a time, the optimum γ	multiple nodes at a time
1	(1.075,0)	(1.34,0.49)	(0.94,0.35)	(0.98,0.17)	(1.09,0)
2	(2.075,0)	(2.33,-0.48)	(2.15,-0.87)	(2.11,-0.83)	(2.02,-0.74)
3	(1.075,2)	(3.33,4.00)	(3.64,3.79)	(3.55,3.86)	(3.48,3.96)
4	(2.075,2)	(1.62,1.55)	(1.47,1.58)	(1.50,1.62)	(1.48,1.36)
5	(1.075,4)	(2.43,3.06)	(2.20,3.90)	(2.18,3.88)	(1.98,3.17)
6	(2.075,4)	(2.28,4.40)	(2.23,4.61)	(2.28,4.66)	(1.79,4.30)
7	(1.075,6)	(1.59,6.73)	(1.96,6.65)	(1.96,6.70)	(2.18,6.70)
8	(2.075,6)	(3.88,5.47)	(3.10,5.80)	(3.13,5.90)	(3.07,5.79)
9	(1.075,8)	(1.30,8.71)	(1.07,7.97)	(1.04,8.07)	(0.96,8.48)
10	(2.075,8)	(2.64,9.22)	(2.47,9.19)	(2.46,9.18)	(2.29,9.39)

Table AppendixC3 The case1 backward positioning result

No. emitter	Position				
	Actual distance	Triangulation	single node at a time,γ =1	single node at a time, the optimum γ	multiple nodes at a time
1	(1.075,0)	(1.72,-0.11)	(0.87,-0.61)	(0.95,-0.42)	(1.01,-0.50)
2	(2.075,0)	(1.64,0.12)	(1.81,0.16)	(1.87,0.18)	(1.96,-0.07)
3	(1.075,2)	(-3.01,-1.22)	(-2.66,-0.62)	(-2.45,-0.30)	(-2.08,1.72)
4	(2.075,2)	(2.87,5.37)	(2.68,4.81)	(2.88,1.37)	(2.85,5.30)
5	(1.075,4)	(2.70,5.59)	(2.78,6.74)	(3.13,5.07)	(2.85,4.46)
6	(2.075,4)	(0.32,2.37)	(1.01,2.76)	(1.50,3.41)	(1.11,1.64)
7	(1.075,6)	(0.80,5.87)	(1.24,5.85)	(1.59,5.80)	(1.07,5.70)
8	(2.075,6)	(3.15,7.18)	(3.08,7.05)	(3.09,6.94)	(3.17,7.19)
9	(1.075,8)	(0.20,7.94)	(0.35,7.87)	(0.30,7.84)	(0.21,7.94)
10	(2.075,8)	(1.80,9.98)	(2.44,10.15)	(2.26,10.01)	(1.60,9.64)

Table AppendixC4 The case1 left-hand side positioning result

	Actual distance	Triangulation	single node at a time,γ =1	single node at a time, the optimum γ	multiple nodes at a time
No.	(1.075,0)	(0.97,-0.33)	(0.97,0.14) Position	(0.97,0.24)	(0.98,0.33)
2	(2.075,0)	(1.62,-0.74)	(1.75,-0.84)	(1.62,-0.98)	(1.52,-1.25)
3	(1.075,2)	(1.84,1.51)	(1.77,1.43)	(1.81,1.47)	(1.68,1.38)
4	(2.075,2)	(2.04,1.04)	(2.07,1.11)	(2.06,1.07)	(1.94,0.80)
5	(1.075,4)	(3.80,5.26)	(2.48,5.04)	(2.91,5.20)	(1.54,5.12)
6	(2.075,4)	(0.76,5.39)	(0.72,5.35)	(0.76,5.41)	(0.28,5.69)
7	(1.075,6)	(1.82,5.99)	(1.19,6.39)	(1.36,6.29)	(1.45,6.09)
8	(2.075,6)	(4.91,4.92)	(5.01,7.22)	(4.96,5.21)	(4.76,5.09)
9	(1.075,8)	(1.40,7.71)	(1.30,8.42)	(1.37,8.06)	(0.97,7.42)
10	(2.075,8)	(2.15,7.70)	(2.30,7.37)	(2.22,7.47)	(1.93,7.54)

Table AppendixC5 The case2 right-hand side positioning result

No. emitter	Position				
	Actual distance	Triangulation	single node at a time,γ =1	single node at a time, the optimum γ	multiple nodes at a time
1	(1.075,0)	(0.75,-0.04)	(1.03,-0.10)	(0.74,-0.10)	(0.80,-0.08)
2	(2.075,0)	(2.25,-0.07)	(2.18,0.10)	(2.24,0.14)	(2.23,0.00)
3	(1.075,2)	(2.15,0.23)	(1.73,0.31)	(2.57,0.12)	(2.10,0.21)
4	(2.075,2)	(3.18,4.00)	(1.85,3.51)	(1.50,3.46)	(3.08,3.88)
5	(1.075,4)	(-0.74,5.97)	(-0.32,6.10)	(-0.11,6.34)	(-0.06,6.40)
6	(2.075,4)	(0.94,4.21)	(0.68,5.69)	(0.72,4.77)	(0.70,5.30)
7	(1.075,6)	(0.09,7.64)	(-0.002, 7.71)	(-0.004, 7.74)	(2.98,-3.58)
8	(2.075,6)	(3.59,5.68)	(4.04,6.08)	(4.13,6.33)	(4.14,6.06)
9	(1.075,8)	(1.84,8.00)	(1.28,8.24)	(0.96,8.23)	(0.98,8.44)
10	(2.075,8)	(-1.07,5.25)	(-0.65,6.11)	(2.15,7.51)	(-0.26,8.21)

Appendix Table C6 The case2 forward positioning result

	Actual distance	Triangulation	single node at a time,γ =1	single node at a time, the optimum γ	multiple nodes at a time
1	(1.075,0)	(1.52,-0.11)	(1.33,-0.15)	(1.53,-0.14)	(1.53,-0.10)
2	(2.075,0)	(1.96,-0.03)	(1.68,-0.09)	(1.79,-0.10)	(1.95,0.13)
3	(1.075,2)	(1.53,0.30)	(1.24,0.27)	(1.36,0.33)	(1.55,0.40)
4	(2.075,2)	(1.20,1.01)	(1.22,0.22)	(1.10,0.22)	(1.38,1.39)
5	(1.075,4)	(-2.32,1.23)	(-0.50,1.07)	(-0.70,1.73)	(-1.58,1.74)
6	(2.075,4)	(2.99,1.04)	(2.26,0.12)	(2.63,0.47)	(2.75,0.98)
7	(1.075,6)	(1.69,3.17)	(2.56,4.14)	(1.60,3.66)	(2.05,3.78)
8	(2.075,6)	(2.33,5.33)	(1.66,5.30)	(1.99,5.35)	(2.10,6.38)
9	(1.075,8)	(2.60,8.19)	(2.80,8.17)	(2.81,8.08)	(2.40,7.85)
10	(2.075,8)	(3.02,7.35)	(3.01,7.38)	(3.01,7.36)	(3.02,7.40)

Appendix Table C7 The case2 backward positioning result

No. emitter	Position				
	Actual distance	Triangulation	single node at a time,γ =1	single node at a time, the optimum γ	multiple nodes at a time
1	(1.075,0)	(1.20,-0.28)	(1.09,-0.05)	(1.56,-0.18)	(1.07,0.02)
2	(2.075,0)	(1.30,-0.11)	(1.58,-0.24)	(1.39,-0.16)	(1.55,-0.27)
3	(1.075,2)	(-2.02,-0.14)	(-1.61,-0.21)	(-2.01,-0.27)	(-2.05,0.31)
4	(2.075,2)	(1.39,0.22)	(1.28,0.35)	(1.36,0.31)	(1.47,0.25)
5	(1.075,4)	(0.22,5.38)	(0.37,4.15)	(0.84,4.48)	(0.15,4.34)
6	(2.075,4)	(-1.01,0.03)	(-1.30,0.63)	(-0.93,0.36)	(-0.96,0.35)
7	(1.075,6)	(0.47,3.63)	(0.81,3.65)	(0.47,3.58)	(0.37,4.12)
8	(2.075,6)	(8.58,3.05)	(8.66,2.40)	(9.74,2.87)	(8.64,5.39)
9	(1.075,8)	(8.17,-0.35)	(8.75,-2.31)	(8.05,-0.29)	(7.95,-0.64)
10	(2.075,8)	(1.98,7.92)	(2.02,8.06)	(2.07,7.89)	(1.89,7.90)

Appendix Table C8 The case2 left-hand side positioning result

No. emitter	Position				
	Actual	Triangulation	single node at	single node at	multiple

	distance		a time,γ =1	a time, the optimum γ	nodes at a time
1	(1.075,0)	(0.57,-0.23)	(0.41,-0.26)	(0.43,-0.29)	(0.25,-0.22)
2	(2.075,0)	(2.96,0.06)	(2.85,0.11)	(2.91,0.05)	(3.07,0.02)
3	(1.075,2)	(0.99,2.37)	(0.74,2.15)	(0.86,2.57)	(0.91,2.09)
4	(2.075,2)	(4.06,10.27)	(3.99,10.22)	(3.97,10.24)	(4.17,10.48)
5	(1.075,4)	(1.89,9.40)	(2.23,8.81)	(1.90,8.94)	(1.83,8.56)
6	(2.075,4)	(3.23,1.92)	(3.18,5.09)	(2.86,4.06)	(2.89,2.14)
7	(1.075,6)	(2.95,7.07)	(2.88,7.09)	(2.86,7.01)	(2.92,7.10)
8	(2.075,6)	(0.56,4.98)	(0.62,5.45)	(0.70,5.05)	(0.80,5.10)
9	(1.075,8)	(2.64,6.49)	(2.94,6.37)	(2.79,6.34)	(2.77,6.30)
10	(2.075,8)	(2.96,7.28)	(3.04,7.02)	(3.02,7.22)	(3.08,7.17)

Appendix Table C9 The case3 right-hand side positioning result

No. emitter	Position				
	Actual distance	Triangulation	single node at a time,γ =1	single node at a time, the optimum γ	multiple nodes at a time
1	(1.075,0)	(1.60,-0.05)	(1.28,0.07)	(1.42,-0.02)	(1.56,-0.06)
2	(2.075,0)	(1.48,0.04)	(1.44,-0.08)	(1.49,-0.10)	(1.44,-0.12)
3	(1.075,2)	(-0.39,3.02)	(-1.57,1.61)	(-1.20,1.73)	(-0.27,3.05)
4	(2.075,2)	(2.34,0.53)	(2.17,0.69)	(2.29,0.46)	(2.33,0.56)
5	(1.075,4)	(2.49,3.04)	(1.47,3.15)	(1.61,3.24)	(2.19,3.08)
6	(2.075,4)	(1.55,3.58)	(2.02,4.44)	(2.06,4.20)	(1.79,3.61)
7	(1.075,6)	(0.40,8.08)	(0.36,7.98)	(0.32,7.96)	(0.38,7.75)
8	(2.075,6)	(2.64,8.16)	(2.48,8.28)	(2.55,8.31)	(3.12,8.02)
9	(1.075,8)	(3.08,8.18)	(2.10,8.82)	(1.90,8.62)	(2.35,8.37)
10	(2.075,8)	(1.42,7.73)	(1.38,8.05)	(1.51,8.04)	(1.73,7.90)

Appendix Table C10 The case3 forward positioning result

No. emitter	Position				
	Actual	Triangulation	single node at	single node	multiple

	distance		a time,γ =1	at a time, the optimum γ	nodes at a time
1	(1.075,0)	(1.54,-0.22)	(1.69,-0.14)	(1.63,-0.11)	(1.50,-0.08)
2	(2.075,0)	(1.91,0.07)	(1.90,0.07)	(1.93,0.06)	(1.92,0.05)
3	(1.075,2)	(1.01,0.97)	(0.71,1.16)	(0.86,1.09)	(0.71,1.23)
4	(2.075,2)	(2.37,0.45)	(2.54,0.67)	(2.52,0.66)	(2.15,0.22)
5	(1.075,4)	(0.95,1.59)	(0.69,2.49)	(1.08,2.51)	(1.03,1.55)
6	(2.075,4)	(2.84,0.93)	(3.76,2.44)	(3.72,1.36)	(2.85,0.87)
7	(1.075,6)	(1.13,2.41)	(1.90,3.08)	(1.58,3.12)	(0.65,2.58)
8	(2.075,6)	(-0.09,4.08)	(0.10,5.85)	(1.06,5.80)	(-0.51,4.11)
9	(1.075,8)	(3.23,7.56)	(3.32,7.68)	(3.24,7.83)	(3.37,7.82)
10	(2.075,8)	(3.35,8.54)	(3.29,9.32)	(3.18,8.72)	(3.34,8.25)

Appendix Table C11 The case3 backward positioning result

No. emitter	Position				
	Actual distance	Triangulation	single node at a time,γ =1	single node at a time, the optimum γ	multiple nodes at a time
1	(1.075,0)	(1.72,-0.53)	(1.43,-0.12)	(1.52,-0.14)	(1.79,-0.49)
2	(2.075,0)	(3.06,0.02)	(3.06,0.05)	(3.06,0.03)	(3.06,0.02)
3	(1.075,2)	(0.39,0.19)	(0.35,-0.25)	(0.42,-0.20)	(0.40,0.17)
4	(2.075,2)	(-0.83,0.86)	(-1.08,0.86)	(-1.07,0.93)	(-0.84,0.82)
5	(1.075,4)	(2.06,1.79)	(1.01,2.83)	(1.21,2.74)	(2.08,1.61)
6	(2.075,4)	(-0.23,3.93)	(-0.53,2.75)	(-0.27,3.44)	(-0.54,3.56)
7	(1.075,6)	(0.29,3.42)	(0.10,4.04)	(0.06,4.08)	(0.32,3.42)
8	(2.075,6)	(1.80,5.03)	(2.86,6.07)	(2.68,6.17)	(1.61,4.92)
9	(1.075,8)	(1.97,8.55)	(-0.77,8.48)	(-0.78,8.49)	(1.93,8.41)
10	(2.075,8)	(2.31,7.31)	(2.01,6.37)	(1.65,6.34)	(2.57,7.84)

Appendix Table C12 The case3 left-hand side positioning result

No. emitter	Position				
	Actual distance	**Triangulation**	**single node at a time,γ =1**	**single node at a time, the optimum γ**	**multiple nodes at a time**
1	(1.075,0)	(1.37,-0.11)	(0.81,-0.03)	(0.79,-0.03)	(0.95,-0.07)
2	(2.075,0)	(2.43,0.39)	(2.27,0.15)	(2.23,0.15)	(2.33,0.20)
3	(1.075,2)	(3.90,3.50)	(1.69,4.41)	(1.62,4.44)	(3.60,3.25)
4	(2.075,2)	(0.84,2.02)	(1.73,3.15)	(1.71,3.19)	(1.27,2.48)
5	(1.075,4)	(0.32,2.39)	(0.19,2.08)	(0.17,2.20)	(0.31,2.36)
6	(2.075,4)	(3.17,3.43)	(2.83,3.45)	(2.86,3.53)	(3.08,3.71)
7	(1.075,6)	(3.82,8.75)	(3.64,8.42)	(3.63,8.42)	(3.88,8.57)
8	(2.075,6)	(2.26,5.10)	(2.23,4.84)	(2.20,4.88)	(2.23,4.83)
9	(1.075,8)	(3.73,9.40)	(3.32,9.02)	(3.25,8.71)	(3.19,9.59)
10	(2.075,8)	(-0.43,12.87)	(3.95,10.19)	(3.46,10.73)	(-1.23,9.55)

CIRRICULUM VITAE

NAME : Ms. Rattikar Punviset

BIRTH DATE : April 7, 1988

BIRTH PLACE : Bangkok, Thailand

EDUCATION :

YEAR	INSTITUTE	DEGREE/DIPLOMA
2010	Kasetsart University	B.Eng. (Electrical Engineering)
2012	Kasetsart University	M.Eng. (Information and Communication Technology for Embedded Systems)

POSITION/TITLE : -

WORK PLACE : -

SCHOLARSHIP/AWARDS : TAIST ICTES Master Degree Scholarship

PUBLICATIONS :

1) Rattikar Punviset , Teerasit Kasetkasem,La-or Kovavisaruch, Tsuyoshi Isshiki.'The Sensor Localization System based on Markov Random Field Model for Stationary Wireless Sensor Network',The Third International Conference of Information and Communication Technology for Embedded Systems (IC-ICTES 2012), Bangkok, Thailand, 22-24 March 2012
2) Rattikar Punviset, Teerasit Kasetkasem,La-or Kovavisaruch, Tsuyoshi Isshiki.'An Optimum Markov Random Field-BasedLocalization Algorithm in Wireless Sensor Networks'.pp.176.In 2012 9th Electical Engineering/Electronics, Computer, Telecommunications and Information Technology, International Conference on. KMUTT, Phetchaburi.